

# New Phenomena in Large-Scale Internet Traffic

Jeremy Kepner,<sup>1\*</sup> Kenjiro Cho,<sup>2</sup> KC Claffy<sup>3</sup>

<sup>1</sup>Lincoln Laboratory Supercomputing Center, Massachusetts Institute of Technology,  
244 Wood Street, Lexington, MA 02421, USA

<sup>2</sup>Research Laboratory, Internet Initiative Japan, Inc.

Iidabashi Grand Bloom, 2-10-2 Fujimi, Chiyoda-ku Tokyo 102-0071, Japan

<sup>3</sup>Center for Applied Internet Data Analysis, University of California at San Diego,  
9500 Gilman Dr., Mail Stop 0505, La Jolla, CA 92093, USA

**The Internet is transforming our society, necessitating a quantitative understanding of Internet traffic. Our team collects and curates the largest publicly available Internet traffic data containing 50 billion packets. Analysis of this streaming data using 10,000 processors in the MIT SuperCloud reveals a new phenomena: the importance of otherwise unseen leaf nodes and isolated links in Internet traffic. Our analysis further shows that a two-parameter modified Zipf-Mandelbrot distribution accurately describes a wide variety of source/destination statistics on moving sample windows ranging from 100,000 to 100,000,000 packets over collections that span years and continents. The measured model parameters distinguish different network streams and the model leaf parameter strongly correlates with the fraction of the traffic in different underlying network topologies.**

## Introduction

Our civilization is now dependent on the Internet, necessitating a scientific understanding of this virtual universe (1, 2), that is made more urgent by the rising influence of adversarial Internet robots (botnets) on society (3, 4). The two largest efforts to capture, curate, and share Internet packet traffic data for scientific analysis are led by our team via the Widely Integrated Distributed Environment (WIDE) project (5) and the Center for Applied Internet Data Analysis (CAIDA) (6). These data have been used for a wide variety of research projects resulting in hundreds of peer-reviewed publications (7), ranging from characterizing the global state of Internet traffic, to specific studies of the prevalence of peer-to-peer filesharing traffic, to testing prototype software designed to stop the spread of Internet worms.

The stochastic network structure of Internet traffic is a core property of great interest to a wide range of Internet stakeholders (2) and network scientists (8). Of particular interest is the probability distribution  $p(d)$  where  $d$  is the degree (or count) of several network quantities, such as source packets, source fan-out, packets over a unique source-destination pair (or link), destination fan-in, and destination packets collected over a specified time intervals (Fig. 1A, Eqs. S3-S9). Amongst the earliest and most widely cited results of virtual Internet topology analysis has been the observation that  $p(d) \propto 1/d^\alpha$  with a model exponent  $1 < \alpha < 3$  for large values of  $d$  (9–11). [Note: in our work network topology refers to the graph theoretic virtual topology of sources and destinations and not the underlying physical topology of the Internet (Table S1).] These early observations demonstrated the importance of a few supernodes in the Internet (Fig. 2A) (12). Measurements of power-laws in Internet data stimulated investigations into a wide range of network phenomena in many domains and lay the foundation for the field of network science (8).

Many Internet models are based on data obtained from crawling the network from a number

of starting points (13). These webcrawls naturally sample the supernodes of the network (12) and their resulting  $p(d)$  are accurately fit at large values of  $d$  by single-parameter power-law models (see fig. S1). However, as we will show, for our streaming samples of the Internet there are other topologies that contribute significant traffic. Characterizing a network by a single power-law exponent provides one view of Internet phenomena, but more accurate and complex models are required to understand the diverse topologies seen in streaming samples of the Internet. Improving model accuracy while also increasing model complexity requires overcoming a number of challenges, including acquisition of larger, rigorously collected data sets (14, 15); the enormous computational cost of processing large network traffic graphs (16–18); careful filtering, binning, and normalization of the data; and fitting of nonlinear models to the data (8, 19).

## Approach

This work overcomes these obstacles to improved model accuracy through several techniques. First, for over a decade we have scientifically collected and curated the largest publicly available Internet packet traffic data sets and this work analyzes the very largest collections in our corpora containing 49.6 billion packets (Table 1). Second, utilizing recent innovations in interactive supercomputing (20, 21), matrix-based graph theory (22, 23), and big data mathematics (fig. S8) (24), we have developed a scalable Internet traffic processing pipeline that runs efficiently on more than 10,000 processors in the MIT SuperCloud (25). This pipeline allows us, for the first time, to process our largest traffic collections as network traffic graphs. Third, since not all packets have both source and destination Internet protocol version 4 (IPv4) addresses, the data have been filtered so that for any chosen time window all data sets have the same number of valid IPv4 packets, denoted  $N_V$  (fig. S2, Eq. S1). All computed probability distributions also use the same binary logarithmic binning to allow for consistent statistical comparison across

data sets (Eq. S11) (8, 19). Fourth, to accurately model the data over the full range of  $d$ , we employ a modified Zipf-Mandelbrot distribution (26–28)

$$p(d; \alpha, \delta) \propto 1/(d + \delta)^\alpha \quad (1)$$

The inclusion of a second model offset parameter  $\delta$  allows the model to accurately fit small values of  $d$ , in particular  $d = 1$ , which has the highest observed probability in these streaming data. The modified Zipf-Mandelbrot model is a special case of the more general saturation/cutoff models used to model a variety of network phenomena (Eq. S13) (8, 19). Finally, nonlinear fitting techniques are used to achieve quality fits over the entire range of  $d$  (Eq. S27). Based on the  $\chi^2$  metric, these non-linear fits favor maximizing error sparsity over minimizing outliers (29–31).

## Results

Figure 1B shows five representative model fits out of the 350 performed on 10 datasets, 5 network quantities, and 7 valid packet windows:  $N_V = 10^5, 3 \times 10^5, 10^6, 3 \times 10^6, 10^7, 3 \times 10^7, 10^8$  (see fig. S5A-J for all 350 fits). The model fits are valid over the entire range of  $d$  and provide parameter estimates with precisions of 0.01. In every case, the high value of  $p(d = 1)$  is indicative of a large contribution from a combination of supernode leaves, core leaves, and isolated links (Fig. 2A). The breadth and accuracy of these data allow detailed comparison of the model parameters. Figure 1C shows the model offset  $\delta$  versus the model exponent  $\alpha$  for all 350 fits. The different collection locations are clearly distinguishable in this model parameter space. The Tokyo collections have smaller offsets and are more tightly clustered than the Chicago collections. Chicago B has a consistently smaller source and link packet model offset than Chicago A. All the collections have source, link, and destination packet model exponents in the relatively narrow  $1.5 < \alpha < 2$  range. The source fan-out and destination fan-

in model exponents are in the broader  $1.5 < \alpha < 2.5$  range and are consistent with the prior literature (19). These results represent an entirely new approach to characterizing Internet traffic that allows the distributions to be projected into a low-dimensional space and enables accurate comparisons among packet collections with different locations, dates, durations, and sizes.

Figure 1C indicates that the distributions of the different collection points occupy different parts of the modified Zipf-Mandelbrot model parameter space. Figure 2A depicts the major topological structures in the network traffic. Isolated links are sources and destinations that each have only one connection (Eqs. S31-S36). The first, second, third, ... supernode is the source or destination with the first, second, third, ... most links (Eqs. S37-S43). The core of a network can be defined in a variety of ways (32, 33). In this work, the network core conveys the concept of a collection of sources and destinations that are not isolated and are multiply connected. The core is defined as the collection of sources and destinations in which every source and destination has more than one connection (Eqs. S44-S50). The core, as computed here, does not include the first five supernodes although only the first supernode is significant, and whether or not the other supernodes are included has minimal impact on the core in these data. The core leaves are sources and destinations that have only one connection to a core source or destination (Eqs. S51-S56).

Figure 2B shows the average relative fractions of sources, total packets, total links, and number of destinations in each of the five topologies for the ten data sets, and seven valid packet windows:  $N_V = 10^5, 3 \times 10^5, 10^6, 3 \times 10^6, 10^7, 3 \times 10^7, 10^8$ . The four projections in Fig. 2B were chosen from fig. S6A-D to highlight the differences in the collection locations. The distinct regions in the various projections shown in Fig. 2B indicate that underlying topological differences are present in the data. The Tokyo collections have much larger supernode leaf components than the Chicago collections. The Chicago collections have much larger core and core leaves components than the Tokyo collections. Chicago A consistently has fewer isolated

links than Chicago B. Comparing the modified Zipf-Mandelbrot model parameters in Fig. 1C and underlying topologies in Fig. 2B suggests that the model parameters are a more compact way to distinguish the network traffic.

Figures 1C and 2B indicate that different collection points produce different model parameters  $\alpha$  and  $\delta$ , and that these collection points also have different underlying topologies. Figure 3 connects the model fits and topology observations by plotting the topology fraction as a function of the model leaf parameter  $1/(1 + \delta)^\alpha$  which corresponds to the relative strength of the distribution at  $p(d = 1)$

$$1/(1 + \delta)^\alpha \propto p(d = 1; \alpha, \delta) \quad (2)$$

The correlations revealed in Fig. 3 suggest that the model leaf parameter strongly correlates with the fraction of the traffic in different underlying network topologies and is a potentially new and beneficial way to characterize networks. Fig. 3 indicates that the fraction of sources, links, and destinations in the core shrinks as the relative importance of the leaf parameter in the source fan-out and destination fan-in increases. In other words, more source and destination leaves means a smaller core. Likewise, the fraction of links and total packets in the supernode leaves grows as the leaf parameter in the link packets and source packets increases. Interestingly, the fraction of sources in the core leaves and isolated links decreases as the leaf parameter in the source and destination packets increases indicating a shift of sources away from the core leaves and isolated links into supernode leaves. Thus, the modified Zipf-Mandelbrot model and its leaf parameter provide a direct connection with the network topology, underscoring the value of having accurate model fits across the entire range of values and in particular for  $d = 1$ .

## Conclusions

Our society critically depends on the Internet for our professional, personal, and political lives. This dependence has rapidly grown much stronger than our comprehension of its underlying

structure, performance limits, dynamics, and evolution. Fundamental characteristics of the Internet are perpetually challenging to research and analyze, and we must admit we know little about what keeps the system stable. As a result, researchers and policymakers deal with a multi-trillion-dollar ecosystem essentially in the dark, and agencies charged with infrastructure protection have little situational awareness regarding global dynamics and operational threats. This paper has presented an analysis of the largest publicly available collection of Internet traffic consisting of 50 billion packets and reveals a new phenomena: the importance of otherwise unseen leaf nodes and isolated links in Internet traffic. Our analysis further shows that a two-parameter modified Zipf-Mandelbrot distribution accurately describes a wide variety of source/destination statistics on moving sample windows ranging from 100,000 to 100,000,000 packets over collections that span years and continents. The measured model parameters distinguish different network streams and the model leaf parameter strongly correlates with the fraction of the traffic in different underlying network topologies. These results represent a significant improvement in Internet modeling accuracy, improve our understanding of the Internet, and show the importance of stream sampling for measuring network phenomena.

## References

1. M. Hilbert and P. López, “The world’s technological capacity to store, communicate, and compute information,” *Science*, p. 1200970, 2011.
2. B. Li, J. Springer, G. Bebis, and M. H. Gunes, “A survey of network flow applications,” *Journal of Network and Computer Applications*, vol. 36, no. 2, pp. 567–581, 2013.
3. H. Allcott and M. Gentzkow, “Social media and fake news in the 2016 election,” *Journal of Economic Perspectives*, vol. 31, no. 2, pp. 211–36, 2017.
4. “[https://www.neosit.com/files/neos\\_distil\\_bad\\_bot\\_report\\_2018.pdf](https://www.neosit.com/files/neos_distil_bad_bot_report_2018.pdf).”

5. K. Cho, K. Mitsuya, and A. Kato, "Traffic data repository at the wide project," in *Proceedings of USENIX 2000 Annual Technical Conference: FREENIX Track*, pp. 263–270, 2000.
6. K. Claffy, "Internet tomography," *Nature, Web Matter*, 1999.
7. "<http://www.caida.org/data/publications/>."
8. A.-L. Barabási *et al.*, *Network science*. Cambridge university press, 2016.
9. A.-L. Barabási and R. Albert, "Emergence of scaling in random networks," *Science*, vol. 286, no. 5439, pp. 509–512, 1999.
10. R. Albert, H. Jeong, and A.-L. Barabási, "Internet: Diameter of the world-wide web," *Nature*, vol. 401, no. 6749, p. 130, 1999.
11. J. Leskovec, J. Kleinberg, and C. Faloutsos, "Graphs over time: densification laws, shrinking diameters and possible explanations," in *Proceedings of the eleventh ACM SIGKDD international conference on Knowledge discovery in data mining*, pp. 177–187, ACM, 2005.
12. J. Cao, Y. Jin, A. Chen, T. Bu, and Z.-L. Zhang, "Identifying high cardinality internet hosts," in *INFOCOM 2009, IEEE*, pp. 810–818, IEEE, 2009.
13. C. Olston, M. Najork, *et al.*, "Web crawling," *Foundations and Trends® in Information Retrieval*, vol. 4, no. 3, pp. 175–246, 2010.
14. A. Soule, A. Nucci, R. Cruz, E. Leonardi, and N. Taft, "How to identify and estimate the largest traffic matrix elements in a dynamic environment," in *ACM SIGMETRICS Performance Evaluation Review*, vol. 32, pp. 73–84, ACM, 2004.
15. Y. Zhang, M. Roughan, C. Lund, and D. L. Donoho, "Estimating point-to-point and point-to-multipoint traffic matrices: an information-theoretic approach," *IEEE/ACM Transactions on Networking (TON)*, vol. 13, no. 5, pp. 947–960, 2005.



16. A. Lumsdaine, D. Gregor, B. Hendrickson, and J. Berry, “Challenges in parallel graph processing,” *Parallel Processing Letters*, vol. 17, no. 01, pp. 5–20, 2007.
17. D. A. Bader, H. Meyerhenke, P. Sanders, and D. Wagner, *Graph partitioning and graph clustering*, vol. 588. American Mathematical Soc., 2013.
18. P. Tune, M. Roughan, H. Haddadi, and O. Bonaventure, “Internet traffic matrices: A primer,” *Recent Advances in Networking*, vol. 1, pp. 1–56, 2013.
19. A. Clauset, C. R. Shalizi, and M. E. Newman, “Power-law distributions in empirical data,” *SIAM review*, vol. 51, no. 4, pp. 661–703, 2009.
20. J. Kepner, *Parallel MATLAB for Multicore and Multinode Computers*. SIAM, 2009.
21. A. Reuther, J. Kepner, C. Byun, S. Samsi, W. Arcand, D. Bestor, B. Bergeron, V. Gadepally, M. Houle, M. Hubbell, *et al.*, “Interactive supercomputing on 40,000 cores for machine learning and data analysis,” *IEEE High Performance Extreme Computing Conference (HPEC)*, 2018.
22. T. G. Kolda and B. W. Bader, “Tensor decompositions and applications,” *SIAM review*, vol. 51, no. 3, pp. 455–500, 2009.
23. J. Kepner and J. Gilbert, *Graph algorithms in the language of linear algebra*. SIAM, 2011.
24. J. Kepner and H. Jananathan, *Mathematics of big data: Spreadsheets, databases, matrices, and graphs*. MIT Press, 2018.
25. V. Gadepally, J. Kepner, L. Milechin, W. Arcand, D. Bestor, B. Bergeron, C. Byun, M. Hubbell, M. Houle, M. Jones, *et al.*, “Hyperscaling internet graph analysis with d4m on the mit supercloud,” *IEEE High Performance Extreme Computing Conference (HPEC)*, 2018.

26. B. Mandelbrot, "An informational theory of the statistical structure of language," *Communication theory*, vol. 84, pp. 486–502, 1953.
27. M. A. Montemurro, "Beyond the zipf–mandelbrot law in quantitative linguistics," *Physica A: Statistical Mechanics and its Applications*, vol. 300, no. 3-4, pp. 567–578, 2001.
28. O. Saleh and M. Hefeeda, "Modeling and caching of peer-to-peer traffic," in *Network Protocols, 2006. ICNP'06. Proceedings of the 2006 14th IEEE International Conference on*, pp. 249–258, IEEE, 2006.
29. D. L. Donoho, "Compressed sensing," *IEEE Transactions on information theory*, vol. 52, no. 4, pp. 1289–1306, 2006.
30. R. Chartrand, "Exact reconstruction of sparse signals via nonconvex minimization," *IEEE Signal Process. Lett.*, vol. 14, no. 10, pp. 707–710, 2007.
31. Z. Xu, X. Chang, F. Xu, and H. Zhang, " $l_{1/2}$  regularization: A thresholding representation theory and a fast solver," *IEEE Transactions on neural networks and learning systems*, vol. 23, no. 7, pp. 1013–1027, 2012.
32. S. E. Schaeffer, "Graph clustering," *Computer science review*, vol. 1, no. 1, pp. 27–64, 2007.
33. A. R. Benson, D. F. Gleich, and J. Leskovec, "Higher-order organization of complex networks," *Science*, vol. 353, no. 6295, pp. 163–166, 2016.
34. A. Mahanti, N. Carlsson, A. Mahanti, M. Arlitt, and C. Williamson, "A tale of the tails: Power-laws in internet measurements," *IEEE Network*, vol. 27, no. 1, pp. 59–64, 2013.

35. M. Kitsak, A. El Mokashfi, S. Havlin, and D. Krioukov, “Long-range correlations and memory in the dynamics of internet interdomain routing,” *PloS one*, vol. 10, no. 11, p. e0141481, 2015.
36. M. Lischke and B. Fabian, “Analyzing the bitcoin network: The first four years,” *Future Internet*, vol. 8, no. 1, p. 7, 2016.

## Acknowledgments

This material is based in part upon work supported by the NSF under grants DMS-1312831, CCF-1533644, and CNS-1513283, DHS cooperative agreement FA8750-18-2-0049, and ASD(R&E) under contract FA8702-15-D-0001. Any opinions, findings, and conclusions or recommendations expressed in this material are those of the authors and do not necessarily reflect the views of the NSF, DHS, or ASD(R&E). All source data can be found at the websites <https://mawi.wide.ad.jp>, specifically

<http://mawi.wide.ad.jp/mawi/ditl/ditl2015/>

<http://mawi.wide.ad.jp/mawi/ditl/ditl2017/>

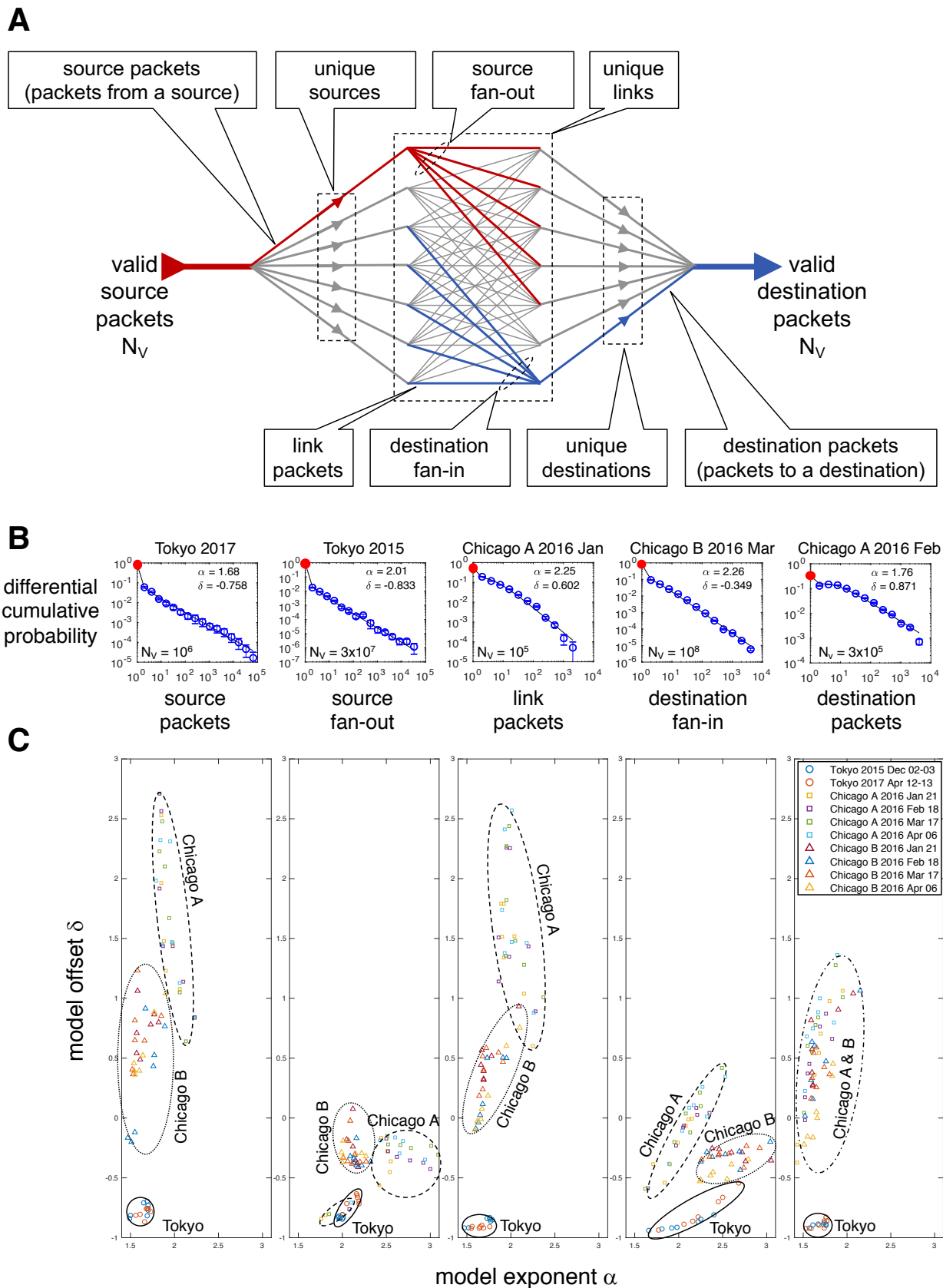
and <https://www.caida.org>, specifically

<https://data.caida.org/datasets/passive-2016/equinix-chicago/>

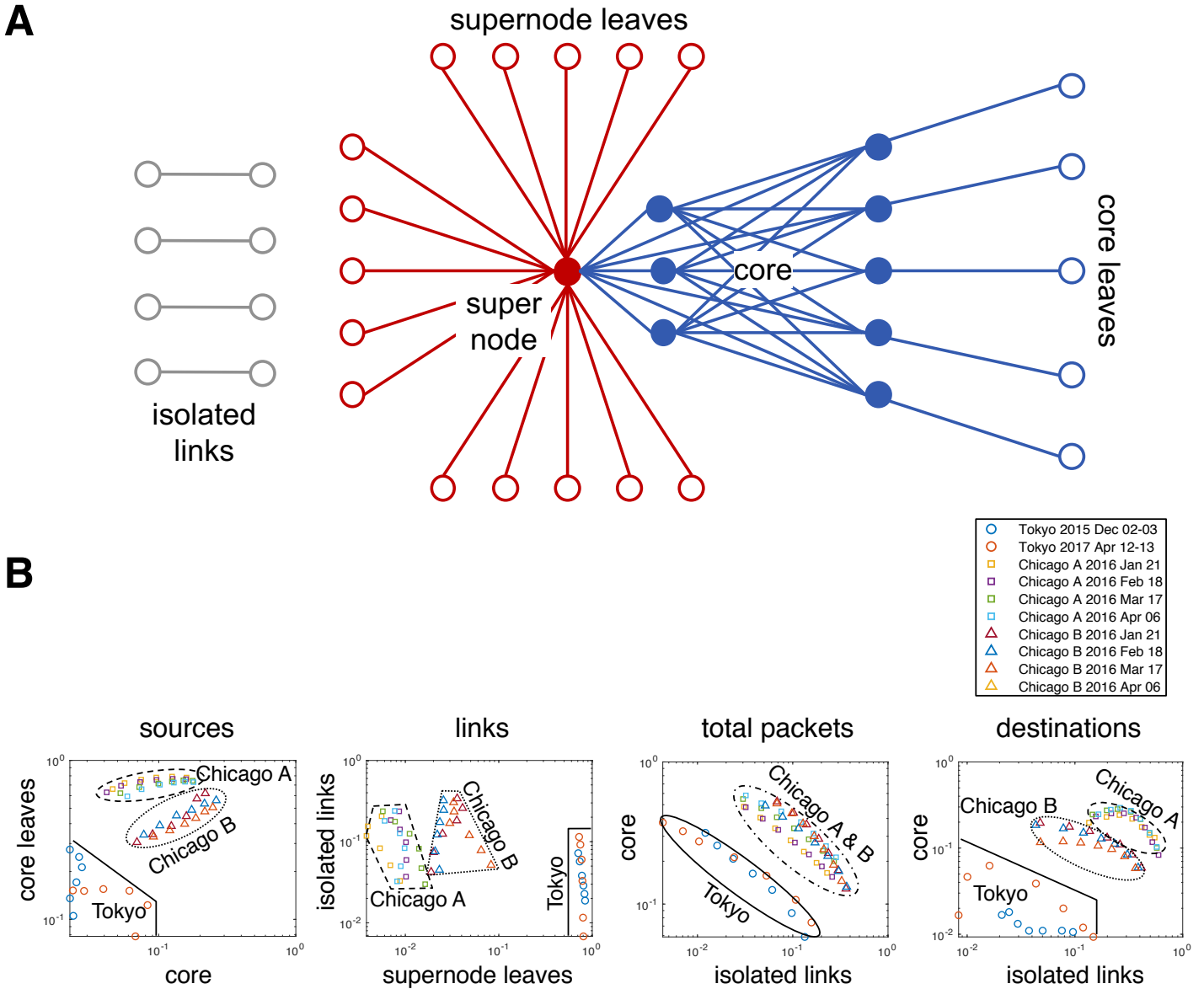
This work used the CAIDA UCSD Anonymized Internet Traces - 2016 January 21, February 18, March 17, and April 06.

Table 1: Large-scale network traffic packet data sets containing 49.6 billion packets collected at different locations, times, and durations over two years.

<b>Location</b>	<b>Date</b>	<b>Duration</b>	<b>Bandwidth</b>	<b>Packets</b>
Tokyo	2015 Dec 02	2 days	$10^9$ bits/sec	$17.0 \times 10^9$
Tokyo	2017 Apr 12	2 days	$10^9$ bits/sec	$16.8 \times 10^9$
Chicago A	2016 Jan 21	1 hour	$10^{10}$ bits/sec	$2.0 \times 10^9$
Chicago A	2016 Feb 18	1 hour	$10^{10}$ bits/sec	$2.0 \times 10^9$
Chicago A	2016 Mar 17	1 hour	$10^{10}$ bits/sec	$1.8 \times 10^9$
Chicago A	2016 Apr 06	1 hour	$10^{10}$ bits/sec	$1.8 \times 10^9$
Chicago B	2016 Jan 21	1 hour	$10^{10}$ bits/sec	$2.3 \times 10^9$
Chicago B	2016 Feb 18	1 hour	$10^{10}$ bits/sec	$1.7 \times 10^9$
Chicago B	2016 Mar 17	1 hour	$10^{10}$ bits/sec	$2.0 \times 10^9$
Chicago B	2016 Apr 06	1 hour	$10^{10}$ bits/sec	$2.1 \times 10^9$



**Figure 1: Streaming network traffic quantities, distributions, and model fits.** (A) Internet traffic streams of  $N_V$  valid packets are divided into a variety of quantities for analysis: source packets, source fan-out, unique source-destination pair packets (or links), destination fan-in, and destination packets. (B) A selection of 5 of the 350 measured differential cumulative probabilities from fig. S5A-J spanning different locations, dates, and packet windows. Blue circles are measured data with  $\pm 1\text{-}\sigma$  error bars. Black lines are the best-fit modified Zipf-Mandelbrot models with parameters  $\alpha$  and  $\delta$ . Red dots highlight the large contribution of leaf nodes and isolated links. (C) Model fit parameters for all 350 measured probability distributions reveal the underlying structural differences among the data collected in Tokyo, Chicago A, and Chicago B.



**Figure 2: Distribution of traffic among network topologies.** (A) Internet traffic forms networks consisting of a variety of topologies: isolated links, supernode leaves connected to a supernode, densely connected core(s) with corresponding core leaves. (B) A selection of four projections from fig. S6A-D showing the fraction of data in various underlying topologies. Horizontal and vertical axis are the corresponding fraction of the sources, links, total packets and destinations that are in various topologies for each location, time, and seven packet windows ( $N_V = 10^5, \dots, 10^8$ ). These data reveal the differences in the network traffic topologies in the data collected in Tokyo (dominated by supernode leaves), Chicago A (dominated by core leaves), and Chicago B (between Tokyo and Chicago A).

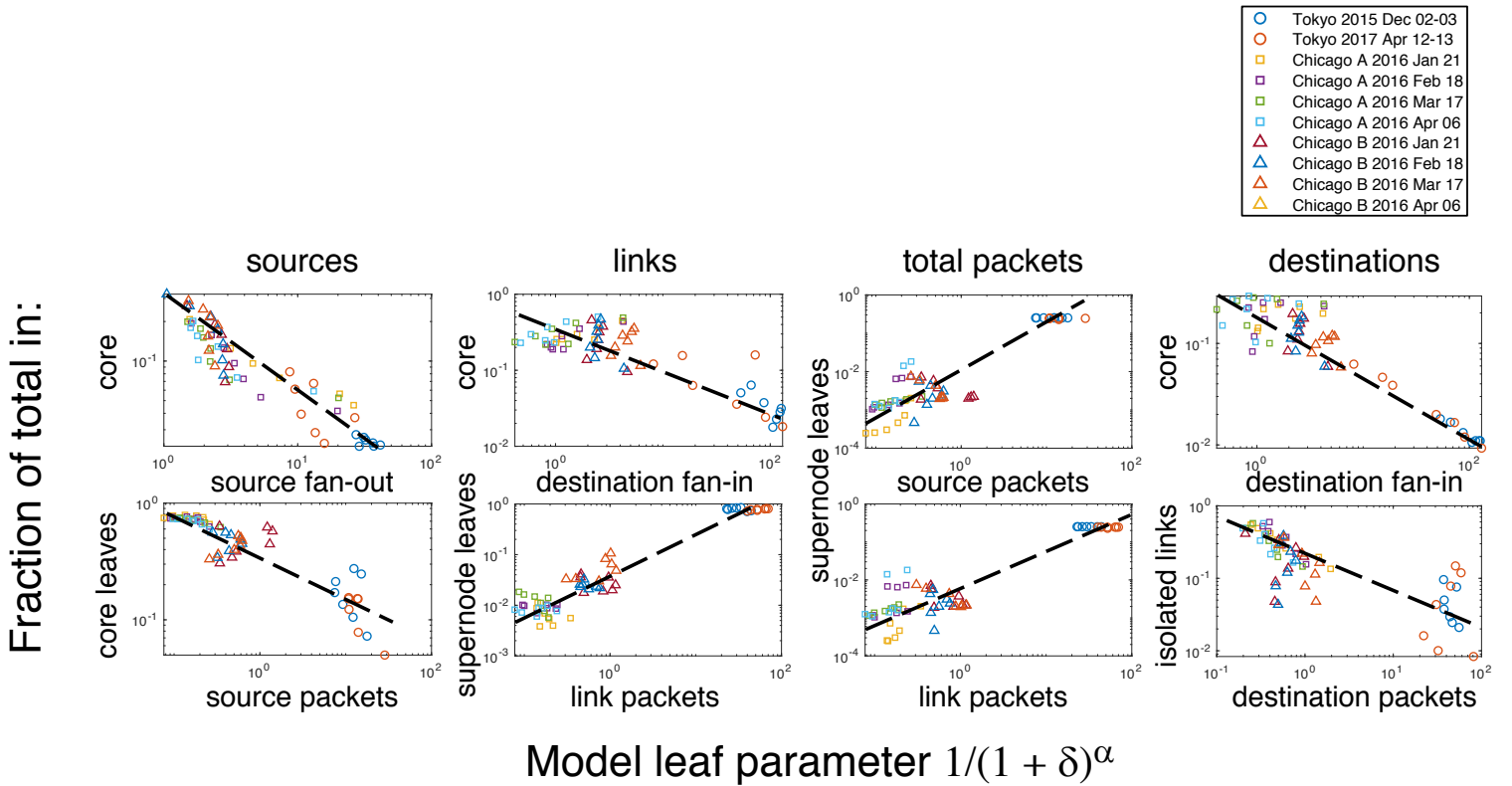


Figure 3: **Topology versus model leaf parameter.** Network topology is highly correlated with the modified Zipf-Mandelbrot model leaf parameter  $1/(1 + \delta)^\alpha$ . A selection of eight projections from fig. S7A-E showing the fraction of data in various underlying topologies. Vertical axis are the corresponding fraction of the sources, links, total packets and destinations that are in various topologies. Horizontal axis is the value of the model parameter taken from either the source packet, source fan-out, link packet, destination fan-in and destination packet fits. Data points are for each location, time, and seven packet windows ( $N_V = 10^5, \dots, 10^8$ ).

# Supplementary Materials for *New Phenomena in Large-Scale Internet Traffic*

Jeremy Kepner, Kenjiro Cho, KC Claffy

## **This supplement includes**

Materials and Methods

Supplementary Text

Figs. S1 to S8

Table S1

References

## **S1 Overview**

This supplement provides further details about the results and analysis that are described in the main text beginning with a review of relevant prior work on Internet analysis. Additional details on the MAWI and CAIDA collection efforts are described. The equations for computing the network quantities and their distributions from matrices are given. Extended results are presented on the consistency of network properties over a wide range of valid packets along with examples of the daily variations observed in the Tokyo data. The equations for the modified Zipf-Mandelbrot model are presented along with the non-linear fitting techniques for computing the model parameters and the complete set of 350 model fits. The equations for computing the different topological components from the matrices are given along with measurements of these topologies in the data. The modified Zipf-Mandelbrot model and the network topologies are shown to be connected through the model's leaf parameter. A description of the memory and computation requirements are provided to show the impact of the MIT SuperCloud capability. Finally, a discussion of the practical implications of this work is provided.



Throughout our work we defer to the terminology of network science. Network operators use many similar terms with significant differences in meaning. We use network topology to refer to the graph theoretic virtual topology of sources and destinations observed communicating and not the underlying physical topology of the Internet (Table S1)

Table S1: Network terminology used by computer network operators and network scientists. Throughout this work the network science meanings are employed.

<b>Term</b>	<b>Network operations meaning</b>	<b>Network science meaning</b>
Network	The <i>physical</i> links, wires, routers, switches, and endpoints used to transmit data.	Any system that can be represented as a <i>graph</i> of connections (links/edges) among entities (nodes/vertices).
Topology	The <i>layout</i> of the physical network.	The specific <i>geometries</i> of a graph and its sub-graphs.
Stream	The <i>flow of data</i> over a specific physical communication link.	A time ordered <i>sequence of pairs</i> of entities (nodes/vertices) representing distinct in time connections (links/edges) between entities.

## S2 Internet Analysis

Quantitative measurements of the Internet (*S1*) have provided Internet stakeholders information on the Internet since its inception. Early work has explored the early growth of the Internet (*S2*), the distribution of packet arrival times (*S3*), the power law distribution of network outages (*S4*), the self-similar behavior of traffic (*S5, S6, S7*), formation processes of power-law networks (*S8, S9, S10, S11*), and the topologies of Internet service providers (*S12*). Subsequent work has examined the technological properties of Internet topologies (*S13*), the diameter of the Internet (*I1*), applying rank index based Zipf-Mandelbrot modeling to peer-to-peer traffic (*28*), and extending topology measurements to edge-hosts (*S14*). More recent work looks to continued measurement of power-law phenomena (*34–36*), exploiting emerging topologies for optimizing

network traffic (*S18, S19, S20*), using network data to locate disruptions (*S21*), the impact of inter-domain congestion (*S22*), and studying the completeness of passive sources to determine how well they can observe microscopic phenomena (*S23*).

The above sample of many years of Internet research has provided significant qualitative insights into Internet phenomenology. Single parameter power-law fits have been explored extensively and shown to adequately fit higher degree tails of the observations. However, more complex models are required to fit the entire range of observations. Fig. S1A adapted from Figure 8H (*I9*) shows the number of bytes of data received in response to  $2.3 \times 10^5$  HTTP (web) requests from computers at a large research laboratory and shows strong agreement with a power-law at large values, but diverges with the single parameter model at small values. Fig. S1B adapted from figure 9W (*I9*) shows the distribution of  $1.2 \times 10^5$  hits on web sites from AOL users and shows strong agreement with a power-law at small values, but diverges with the single parameter model at large values. Fig. S1C adapted from figure 9X (*I9*) shows the distribution of  $2.4 \times 10^8$  web hyperlinks and has reasonable model agreement across the entire range, except for the smallest values. Fig. S1D adapted from figure 4B (*34*) shows the distribution of visitors arriving at YouTube from referring web sites appears to be best represented by two very different power-law models with significant difference as the smallest values. Fig. S1E adapted from figure 3A (*35*) shows the distribution of the number of border gateway protocol updates received by the 4 monitors in 1 minute intervals and shows strong agreement with a power-law at large values, but diverges with the single parameter model at small values. Fig. S1F adapted from figure 21 in (*36*) shows the distribution of the Bitcoin network in 2011 and shows strong agreement with a power-law at small values, but diverges with the single parameter model at large values.

The results shown in fig. S1 represent some of the best and most carefully executed fits to Internet data and clearly show the difficulty of fitting the entire range with a single parameter

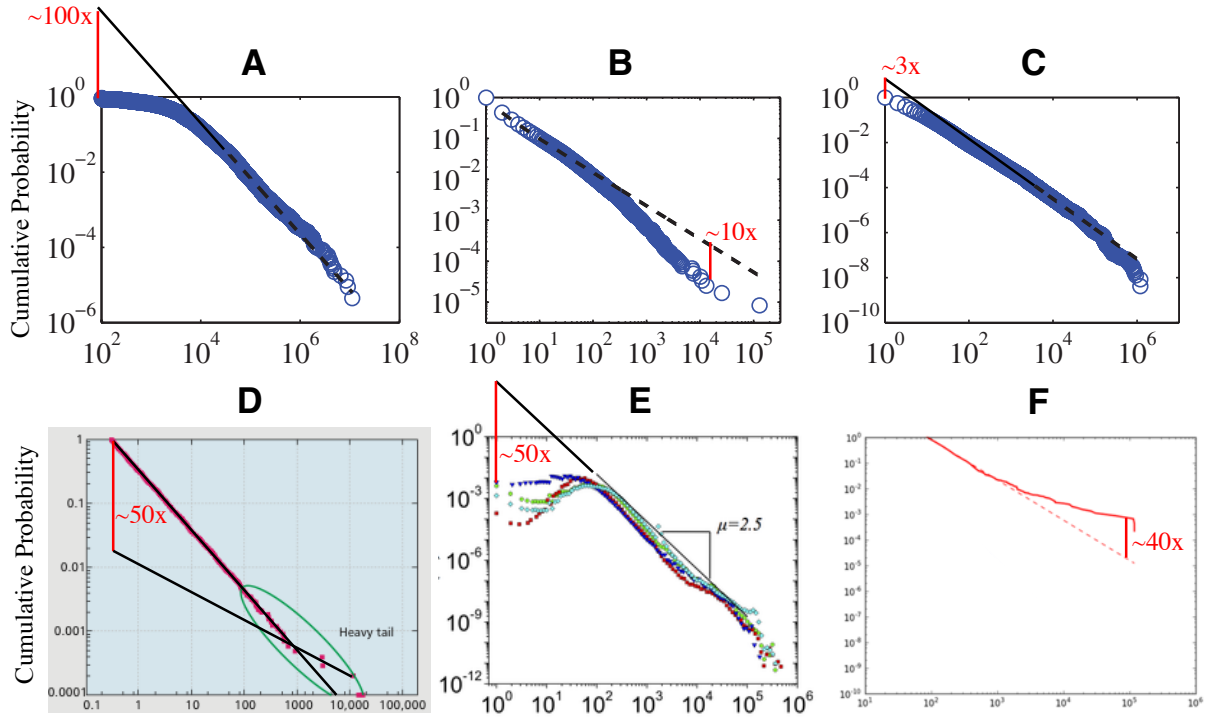


Figure S1: **Single Parameter Power Law Fits of Internet Data.** Single parameter fits of the cumulative distributions of Internet data have difficulty modeling the entire range. The estimated ratio between the model and the data at the model extremes is highlighted in red. (A) Figure 8H (19). (B) Figure 9W (19). (C) Figure 9X (19). (D) Figure 4B (34). (E) Figure 3A (35). (F) Figure 21 (36).

power-law. It is also worth mentioning that in each case the cumulative distribution is used which naturally provides a smoother curve (in contrast to the differential cumulative distribution used in our analysis), but provides less detail on the underlying phenomena. Furthermore the data in fig. S1 are typically isolated collections such that the error bars are not readily computable, which limits the ability to assess both the quality of the measurements and the model fits.

Regrettably, the best publicly available data about the global interconnection system that carries most of the world’s communications traffic is incomplete and of unknown accuracy. There is no map of physical link locations, capacity, traffic, or interconnection arrangements.

This opacity of the Internet infrastructure hinders research and development efforts to model network behavior and topology; design protocols and new architectures; and study real-world properties such as robustness, resilience, and economic sustainability. There are good reasons for the dearth of information: complexity and scale of the infrastructure; information-hiding properties of the routing system; security and commercial sensitivities; costs of storing and processing the data; and lack of incentives to gather or share data in the first place, including cost-effective ways to use it operationally. But understanding the Internet’s history and present, much less its future, is impossible without realistic and representative datasets and measurement infrastructure on which to support sustained longitudinal measurements as well as new experiments. The MAWI and CAIDA data collection efforts are the largest efforts to provide the data necessary to begin to answer these questions.

### **S3 MAWI Internet Traffic Collection**

The WIDE project is a research consortium in Japan established in 1988 (5). The members of the project include network engineers, researchers, university students, and industrial partners. The focus of WIDE is on the empirical study of the large-scale internet. WIDE operates an internet testbed for both commercial traffic and for conducting research experiments. These data have enabled quantitative analysis of Internet traffic spanning years illustrating trends such as, the emergence of residential usage, peer-to-peer networks, probe scanning, and bot-nets (S24, S25, S26). The Tokyo datasets are publicly available packet traces provided by the WIDE project (a.k.a. the MAWI traces). The traces are collected from a 1 Gbps academic backbone connection in Japan. The 2015 and 2017 datasets are 48-hour-long traces captured during December 2-3 2015 and April 12-13 2017 in JST. The IP addresses appearing in the traces are anonymized using a prefix-preserving method (S27).

The MAWI repository is an on-going collection of Internet traffic traces, captured within

the WIDE backbone network (AS2500) that connects Japanese universities and research institutes to the Internet. Each trace consists of captured packets observed from within WIDE, and includes the packet headers of each packet along with the captured timestamp. Anonymized versions of the traces (with anonymized IP addresses and with transport layer payload removed) are made publicly available at <http://mawi.wide.ad.jp/>.

WIDE carries a variety of traffic including academic and commercial traffic. These data have enabled quantitative analysis of Internet traffic spanning years illustrating trends such as the emergence of residential usage, peer-to-peer networks, probe scanning, and botnets (*S24, S28, S26*). WIDE is mostly dominated by HTTP protocol traffic, but is influenced by global anomalies. For example, Code Red, Blaster and Sasser are worms that disrupted Internet traffic (*S29*). Of these, Sasser (2005) impacted MAWI traffic the most, accounting for two-thirds of packets at its peak. Conversely, the ICMP traffic surge in 2003, and the SYN Flood in 2012, were more local in nature, each revealing attacks on targets within WIDE that lasted several months.

## **S4 CAIDA Internet Traffic Collection**

CAIDA collects several different data types at geographically and topologically diverse locations, and makes this data available to the research community to the extent possible while preserving the privacy of individuals and organizations who donate data or network access (*6*) (*S30*). CAIDA has (and had) monitoring locations in Internet Service Providers (ISPs) in the United States. CAIDA's passive traces dataset contains traces collected from high-speed monitors on a commercial backbone link. The data collection started in April 2008 and is ongoing. These data are useful for research on the characteristics of Internet traffic, including application breakdown (based on TCP/IP ports), security events, geographic and topological distribution, flow volume and duration. For an overview of all traces see the trace statistics page (*S31*).

Collectively, our consortium has enabled scientific analysis of Internet traffic resulting in hundreds of peer-reviewed publications with over 30,000 citations (7). These include early work on Internet threats such as the Code-Red worm (*S32*) and Slammer worm (*S33*) and how quarantining might mitigate threats (*S34*). Subsequent work explored various techniques, such as dispersion, for measuring Internet capacity and bandwidth (*S35, S36, S37*). The next major area of research provided significant results on the dispersal of the Internet via the emergence of peer-to-peer networks (*S38, S39*), edge devices (*S40*), and corresponding denial-of-service attacks (*S41*), which drove the need for new ways to categorize traffic (*S42*). Incorporation of network science and statistical physics concepts into the analysis of the Internet produced new results on the hyperbolic geometry of complex networks (*S43, S44*) and sustaining the Internet with hyperbolic mapping (*S45, S46, S47*). Likewise, new understanding also emerged on identification of influential spreaders in complex networks (*S48*), the relationship of popularity versus similarity in growing networks (*S49*), and overall network cosmology (*S50*). More recent work has developed new ideas for Internet classification (*S51*) and future data centric architectures (*S52*).

The traffic traces used in this paper are anonymized using CryptoPan prefix-preserving anonymization. The anonymization key changes annually and is the same for all traces recorded during the same calendar year. During capture packets are truncated at a snap length selected to avoid excessive packet loss due to disk I/O overload. The snap length has historically varied from 64 to 96 bytes. In addition, payload is removed from all packets: only header information up to layer 4 (transport layer) remains. Endace network cards used to record these traces provide timestamps with nanosecond precision. However, the anonymized traces are stored in pcap format with timestamps truncated to microseconds. Starting with the 2010 traces the original nanosecond timestamps are provided as separate ascii files alongside the packet capture files.

## S5 Network Quantities from Matrices

Origin-destination traffic matrices are one of the most generally useful representations of Internet traffic (14,18). These matrices can be used to compute a wide range of network statistics useful in the analysis, monitoring, and control of the Internet. Such analysis include the temporal fluctuations of the supernodes (14) and inferring the presence of unobserved traffic (15) (S53). At a given time  $t$ ,  $N_V$  consecutive valid packets are aggregated from the traffic into a sparse matrix  $\mathbf{A}_t$ , where  $\mathbf{A}_t(i, j)$  is the number of valid packets between the source  $i$  and destination  $j$  (S54). The sum of all the entries in  $\mathbf{A}_t$  is equal to  $N_V$

$$\sum_{i,j} \mathbf{A}_t(i, j) = N_V \quad (\text{S1})$$

All the network quantities depicted in Fig. 1A can be readily computed from  $\mathbf{A}_t$  (Eqs. S2-S9), along with many other network statistics (14, 15, 18).

An essential step for increasing the accuracy of the statistical measures of Internet traffic is using windows with the same number of valid packets  $N_V$ . For this analysis, a valid packet is defined as TCP over IPv4, which includes more than 95% of the data in the collection and eliminates a small amount of data that uses other protocols or contains anomalies. Using packet windows with the same number of valid packets produces quantities that are consistent over a wide range from  $N_V = 100,000$  to  $N_V = 100,000,000$  (fig. S2).

The network quantities depicted in Fig. 1 can be computed from  $\mathbf{A}_t(i, j)$  as follows. The total number of valid packets is the sum of all entries in  $\mathbf{A}_t$

$$\sum_{i,j} \mathbf{A}_t(i, j) = \mathbf{1}^\top \mathbf{A}_t \mathbf{1} = N_V \quad (\text{S2})$$

where  $\mathbf{1}$  is a column vector of all 1's and  $^\top$  is the transpose operation. Adding up the entries in each row of  $\mathbf{A}_t$  produces a column vector of source packets (packets coming from a specific

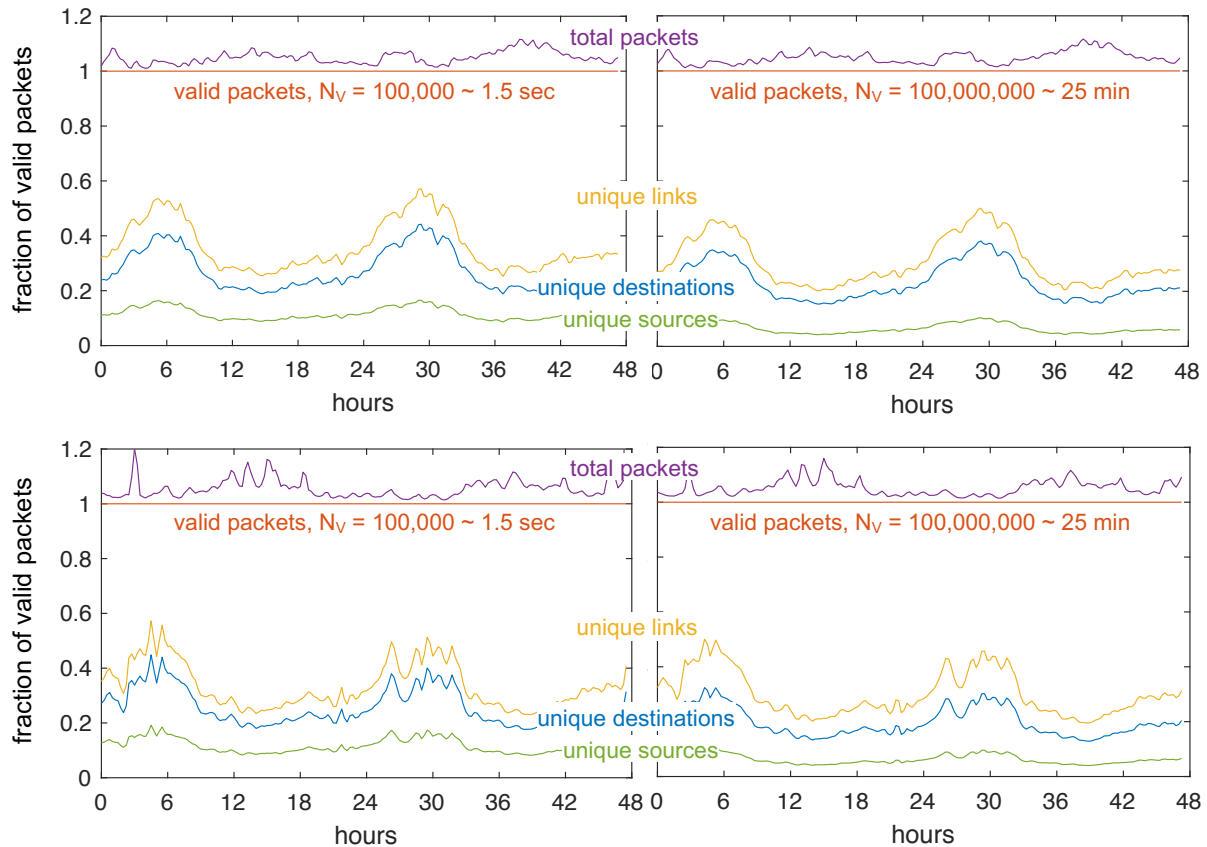


Figure S2: **Valid packets.** Analyzing packet windows with the same numbers of valid packets produces consistent fractions of unique links, unique destinations, and unique sources over a wide range of packet sizes for the Tokyo 2015 (top) and Tokyo 2017 (bottom) data sets. The plots show these fractions for moving packet windows of with  $N_V = 100,000$  packets (left) and  $N_V = 100,000,000$  packets (right). The packet windows correspond to time windows of approximately 1.5 seconds and 25 minutes.



source)

$$\mathbf{A}_t \mathbf{1} \tag{S3}$$

Counting the non-empty rows in  $\mathbf{A}_t$  computes the total number of sources

$$\mathbf{1}^\top |\mathbf{A}_t|_0 \mathbf{1} \tag{S4}$$

where  $|\cdot|_0$  is the zero-norm that sets each nonzero value of its argument to 1 (S55). A row vector of source fan-outs (number of destinations from a given source) is obtained by summing the number nonzero entries in each row

$$|\mathbf{A}_t|_0 \mathbf{1} \tag{S5}$$

The total number of unique links (unique source and destination pairs) is the number of nonzero entries in  $\mathbf{A}_t$

$$\mathbf{1}^\top |\mathbf{A}_t|_0 \mathbf{1} \tag{S6}$$

Counting the nonzero entries in each column produces a row vector of destination fan-ins (number of sources going to a given destination)

$$\mathbf{1}^\top |\mathbf{A}_t|_0 \tag{S7}$$

Counting the non-empty columns in  $\mathbf{A}_t$  computes the total number of destinations

$$|\mathbf{1}^\top \mathbf{A}_t|_0 \mathbf{1} \tag{S8}$$

Adding up the entries in each column of  $\mathbf{A}_t$  produces a row vector of destination packets (packets going to a specific destination)

$$\mathbf{1}^\top \mathbf{A}_t \tag{S9}$$

## S6 Probability Distributions

For a network quantity  $d$ , the histogram of this quantity computed from  $\mathbf{A}_t$  is denoted by  $n_t(d)$ , with corresponding probability

$$p_t(d) = n_t(d) / \sum_d n_t(d) \quad (\text{S10})$$

and cumulative probability

$$P_t(d) = \sum_{i=1,d} p_t(d) \quad (\text{S11})$$

Because of the relatively large values of  $d$  observed due to a single supernode, the measured probability at large  $d$  often exhibits large fluctuations. However, the cumulative probability lacks sufficient detail to see variations arounds specific values of  $d$ , so it is typical to use the differential cumulative probability with logarithmic bins in  $d$

$$D_t(d_i) = P_t(d_i) - P_t(d_{i-1}) \quad (\text{S12})$$

where  $d_i = 2^i$  (19). The corresponding mean and standard deviation of  $D_t(d_i)$  over many different consecutive values of  $t$  for a given data set are denoted  $D(d_i)$  and  $\sigma(d_i)$ . These quantities strike a balance between accuracy and detail for subsequent model fitting as demonstrated in the daily structural variations revealed in the Tokyo data (figs. S3-S4).

## S7 Daily Variations

Diurnal variations in supernode network traffic are well known (14). The Tokyo packet data were collected over a period spanning two days, and allow the daily variations in packet traffic to be observed. The precision and accuracy of our measurements allows these variations to be observed across a wide range of nodes. Figure S3 shows the fraction of source fan-outs in each of various bin ranges. The fluctuations show the network evolving between two envelopes occurring between noon and midnight that are shown in fig. S4.

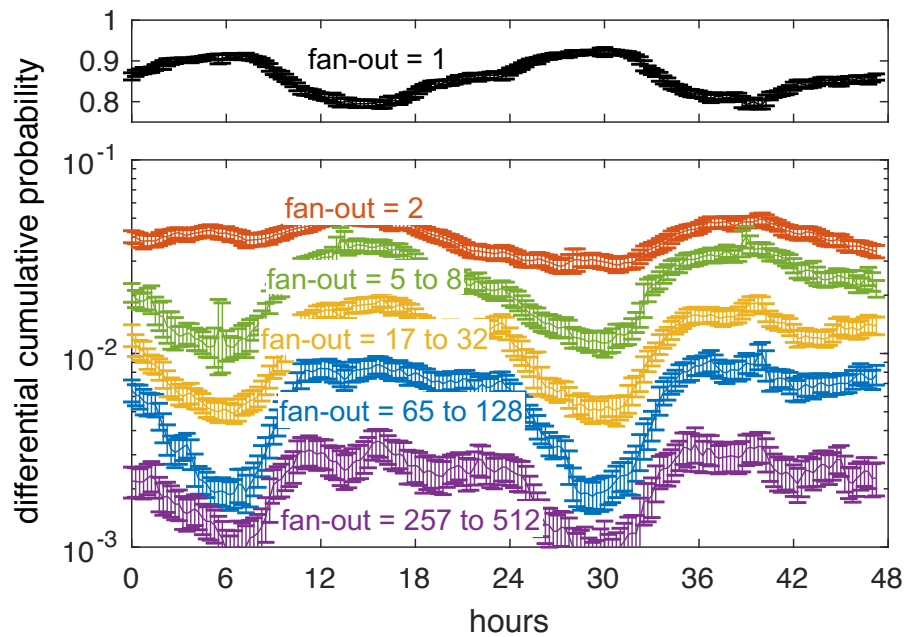


Figure S3: **Daily variation in Internet traffic.** The fraction of source nodes with a given range of fan-out are shown as a function of time for the Tokyo 2015 data. The  $p(d = 1)$  value is plotted on a separate linear scale because of the larger magnitude relative to the other points. Each point is the mean of many neighboring points in time and the error bars are the measured  $\pm 1\sigma$ . The daily variation of the distributions oscillate between extremes corresponding to approximately local noon and midnight.

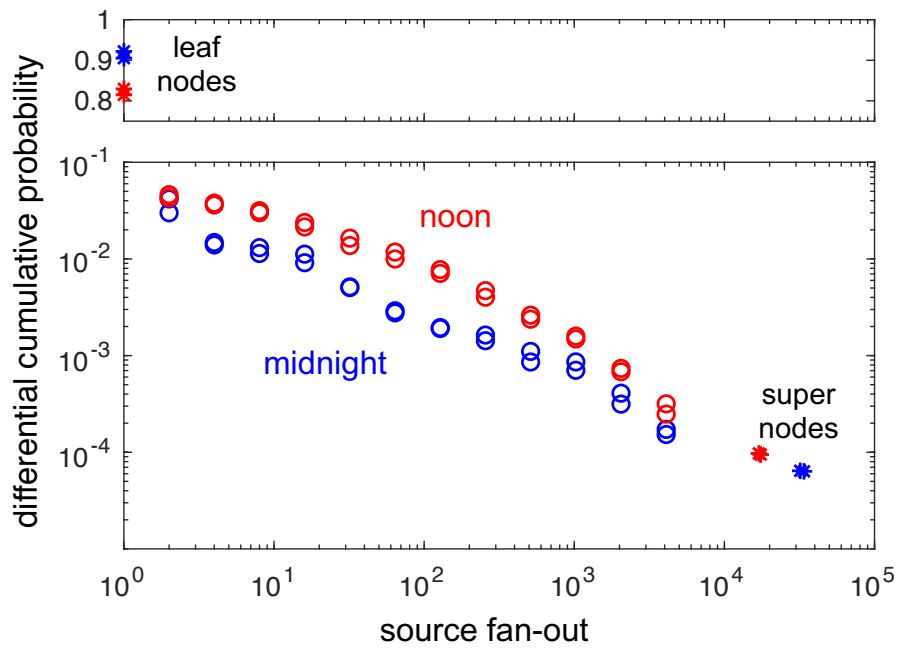


Figure S4: **Daily limits in Internet traffic.** The fraction of source nodes versus fan-out are shown for two noons and two midnights for the Tokyo 2015 data. The overlap among the noons and the midnights shows the relative day-to-day consistency in these data and show the limits of the two extremes in daily variation. During the day, there is more traffic among nodes with intermediate fan-out. At night the traffic is more dominated by leaf nodes and the supernode.

## S8 Modified Zipf-Mandelbrot Model

Measurements of  $D(d_i)$  can reveal many properties of network traffic, such as the number of nodes with only one connection  $D(d = 1)$  and the size of the supernode  $d_{\max} = \operatorname{argmax}(D(d) > 0)$ . An effective low parameter model allows these and many other properties to be summarized and computed efficiently. In the standard Zipf-Mandelbrot model typically used in linguistic contexts, the value  $d$  in Eq. 2 is a ranking with  $d = 1$  corresponding to the most popular value (26–28). In our analysis, the Zipf-Mandelbrot model is modified so that  $d$  is a measured network quantity instead of a rank index (Eq.2). The model exponent  $\alpha$  has a larger impact on the model at large values of  $d$  while the model offset  $\delta$  has a larger impact on the model at small values of  $d$  and in particular at  $d = 1$ .

The general saturation/cutoff models used to model a variety of network phenomena is denoted (8, 19)

$$p(d) \propto \frac{1}{(d + \delta)^\alpha \exp[\lambda d]} \quad (\text{S13})$$

where  $\delta$  is the low- $d$  saturation and  $1/\lambda$  is the high- $d$  cutoff that bounds the power-law regime of the distribution. The modified Zipf-Mandelbrot is a special case of this distribution that accurately models our observations. The unnormalized modified Zipf-Mandelbrot model is denoted

$$\rho(d; \alpha, \delta) = \frac{1}{(d + \delta)^\alpha} \quad (\text{S14})$$

with correspond derivative with respect to  $\delta$

$$\partial_\delta \rho(d; \alpha, \delta) = \frac{-\alpha}{(d + \delta)^{\alpha+1}} = -\alpha \rho(d; \alpha + 1, \delta) \quad (\text{S15})$$

The normalized model probability is given by

$$p(d; \alpha, \delta) = \frac{\rho(d; \alpha, \delta)}{\sum_{d=1}^{d_{\max}} \rho(d; \alpha, \delta)} \quad (\text{S16})$$

where  $d_{max}$  is the largest value of the network quantity  $d$ . The cumulative model probability is the sum

$$P(d_i; \alpha, \delta) = \sum_{d=1}^{d_i} p(d; \alpha, \delta) \quad (\text{S17})$$

The corresponding differential cumulative model probability is

$$D(d_i; \alpha, \delta) = P(d_i; \alpha, \delta) - P(d_{i-1}; \alpha, \delta) \quad (\text{S18})$$

where  $d_i = 2^i$ . In terms of  $\rho$  the differential cumulative model probability is

$$D(d_i; \alpha, \delta) = \frac{\sum_{d=d_{i-1}+1}^{d=d_i} \rho(d; \alpha, \delta)}{\sum_{d=1}^{d=d_{max}} \rho(d; \alpha, \delta)} \quad (\text{S19})$$

The above function is closely related to the Hurwitz-Zeta function (S57, S59, 19)

$$\zeta(\alpha, \delta_1) = \sum_{d=0}^{\infty} \rho(d; \alpha, \delta_1) \quad (\text{S20})$$

where  $\delta_1 = \delta + 1$ . The differential cumulative model probability in terms of the Hurwitz-Zeta function is

$$D(d_i; \alpha, \delta) = \frac{\zeta(\alpha, \delta + 3 + d_{i-1}) - \zeta(\alpha, \delta + 2 + d_i)}{\zeta(\alpha, \delta+) - \zeta(\alpha, \delta+)} \quad (\text{S21})$$

## S9 Nonlinear Model Fitting

The model exponent  $\alpha$  has a larger impact on the model at large values of  $d$  while the model offset  $\delta$  has a larger impact on the model at small values of  $d$  and in particular at  $d = 1$ . A nonlinear fitting technique is used to obtain accurate model fits across the entire range of  $d$ . Initially, a set of candidate exponent values is selected, typically  $\alpha = 0.10, 0.11, \dots, 3.99, 4.00$ . For each value of  $\alpha$ , a value of  $\delta$  is computed that exactly matches the model with the data at  $D(1)$ . Finding the value of  $\delta$  corresponding to a give  $D(1)$  is done using Newton's method as follows. Setting the measured value of  $D(1)$  equal to the model value  $D(1; \alpha, \delta)$  gives

$$D(1) = D(1; \alpha, \delta) = \frac{1}{(1 + \delta)^\alpha \sum_{d=1}^{d_{max}} \rho(d; \alpha, \delta)} \quad (\text{S22})$$

Newton's method works on functions of the form  $f(\delta) = 0$ . Rewriting the above expression produces

$$f(\delta) = D(1)(1 + \delta)^\alpha \sum_{d=1}^{d_{\max}} \rho(d; \alpha, \delta) - 1 = 0 \quad (\text{S23})$$

For given value of  $\alpha$ ,  $\delta$  can be computed from the following iterative equation

$$\delta \rightarrow \delta - \frac{f(\delta)}{\partial_\delta f(\delta)} \quad (\text{S24})$$

where the partial derivative  $\partial_\delta f(\delta)$  is

$$\begin{aligned} \partial_\delta f(\delta) &= D(1) \partial_\delta [(1 + \delta)^\alpha \sum_{d=1}^{d_{\max}} \rho(d; \alpha, \delta)] \\ &= D(1) [\alpha(1 + \delta)^{\alpha-1} \sum_{d=1}^{d_{\max}} \rho(d; \alpha, \delta) + [(1 + \delta)^\alpha \sum_{d=1}^{d_{\max}} \partial_\delta \rho(d; \alpha, \delta)]] \\ &= D(1) [\alpha(1 + \delta)^{\alpha-1} \sum_{d=1}^{d_{\max}} \rho(d; \alpha, \delta) + [(1 + \delta)^\alpha \sum_{d=1}^{d_{\max}} -\alpha \rho(d; \alpha + 1, \delta)]] \\ &= \alpha D(1) (1 + \delta)^\alpha [(1 + \delta)^{-1} \sum_{d=1}^{d_{\max}} \rho(d; \alpha, \delta) - \sum_{d=1}^{d_{\max}} \rho(d; \alpha + 1, \delta)] \end{aligned} \quad (\text{S25})$$

Using a starting value of  $\delta = 1$  and bounds of  $0 < \delta < 10$ , Newton's method can be iterated until the differences in successive values of  $\delta$  fall below a specified error (typically 0.001) and is usually achieved in less than five iterations.

If faster evaluation is required, the sums in the above formulas can be accelerated using the integral approximations

$$\begin{aligned} \sum_{d=1}^{d_{\max}} \rho(d; \alpha, \delta) &\approx \sum_{d=1}^{d_{\text{sum}}} \rho(d; \alpha, \delta) + \int_{d_{\text{sum}}+0.5}^{d_{\max}+0.5} \rho(x; \alpha, \delta) dx \\ &= \sum_{d=1}^{d_{\text{sum}}} \rho(d; \alpha, \delta) + \frac{\rho(d_{\text{sum}} + 0.5; \alpha - 1, \delta) - \rho(d_{\max} + 0.5; \alpha - 1, \delta)}{\alpha - 1} \\ \sum_{d=1}^{d_{\max}} \rho(d; \alpha + 1, \delta) &\approx \sum_{d=1}^{d_{\text{sum}}} \rho(d; \alpha + 1, \delta) + \int_{d_{\text{sum}}+0.5}^{d_{\max}+0.5} \rho(x; \alpha + 1, \delta) dx \\ &= \sum_{d=1}^{d_{\text{sum}}} \rho(d; \alpha + 1, \delta) + \frac{\rho(d_{\text{sum}} + 0.5; \alpha, \delta) - \rho(d_{\max} + 0.5; \alpha, \delta)}{\alpha} \end{aligned} \quad (\text{S26})$$

where the parameter  $d_{\text{sum}}$  can be adjusted to exchange speed for accuracy. For typical values of  $\alpha$ ,  $\delta$ , and  $d_{\text{max}}$  used in this work, the accuracy is approximately  $1/d_{\text{sum}}$ .

The best-fit  $\alpha$  (and corresponding  $\delta$ ) is chosen by minimizing the  $|\cdot|^{1/2}$  metric over logarithmic differences between the candidate models  $D(d_i; \alpha, \delta)$  and the data

$$\operatorname{argmin}_{\alpha} \sum_{d_i} |\log(D(d_i)) - \log(D(d_i; \alpha, \delta))|^{1/2} \quad (\text{S27})$$

The  $|\cdot|^{1/2}$  metric (or  $|\cdot|_p$ -norm with  $p = 1/2$ ) favors maximizing error sparsity over minimizing outliers (29–31) (S55, S60, S61, S62). Several authors have shown recently that it is possible to reconstruct a nearly sparse signal from fewer linear measurements than would be expected from traditional sampling theory. Furthermore, by replacing the  $|\cdot|_1$  norm with the  $|\cdot|_p$  with  $p < 1$ , reconstruction is possible with substantially fewer measurements.

Using logarithmic values more evenly weights their contribution to the model fit and more accurately reflects the number of packets used to compute each value of  $D(d_i)$ . Lower accuracy data points are avoided by limiting the fitting procedure to data points where the value is greater than the standard deviation:  $D(d_i) > \sigma(d_i)$ .



## S10 Measured Distributions and Model Fits

Figure S5A-J shows the measured and modeled differential cumulative distributions for the source fan-out, source packets, destination fan-in, destination packets, and link packets for all the collected data.

Figure S5: **Complete data and model fits.** 350 measured differential cumulative probabilities (blue circles with  $\pm 1\text{-}\sigma$  error bars) along with their best-fit modified Zipf-Mandelbrot models (black line) and parameters  $\alpha$  and  $\delta$  performed on ten data sets, five network quantities, and seven valid packet windows:  $N_V = 10^5, 3 \times 10^5, 10^6, 3 \times 10^6, 10^7, 3 \times 10^7, 10^8$ .

(A) Tokyo 2015 Dec 02.

(B) Tokyo 2017 Apr 12.

(C) Chicago A 2016 Jan 21.

(D) Chicago A 2016 Feb 18.

(E) Chicago A 2016 Mar 17.

(F) Chicago A 2016 Apr 06.

(G) Chicago B 2016 Jan 21.

(H) Chicago B 2016 Feb 18.

(I) Chicago B 2016 Mar 17.

(J) Chicago B 2016 Apr 06.

valid packets: 100,000

300,000

1,000,000

3,000,000

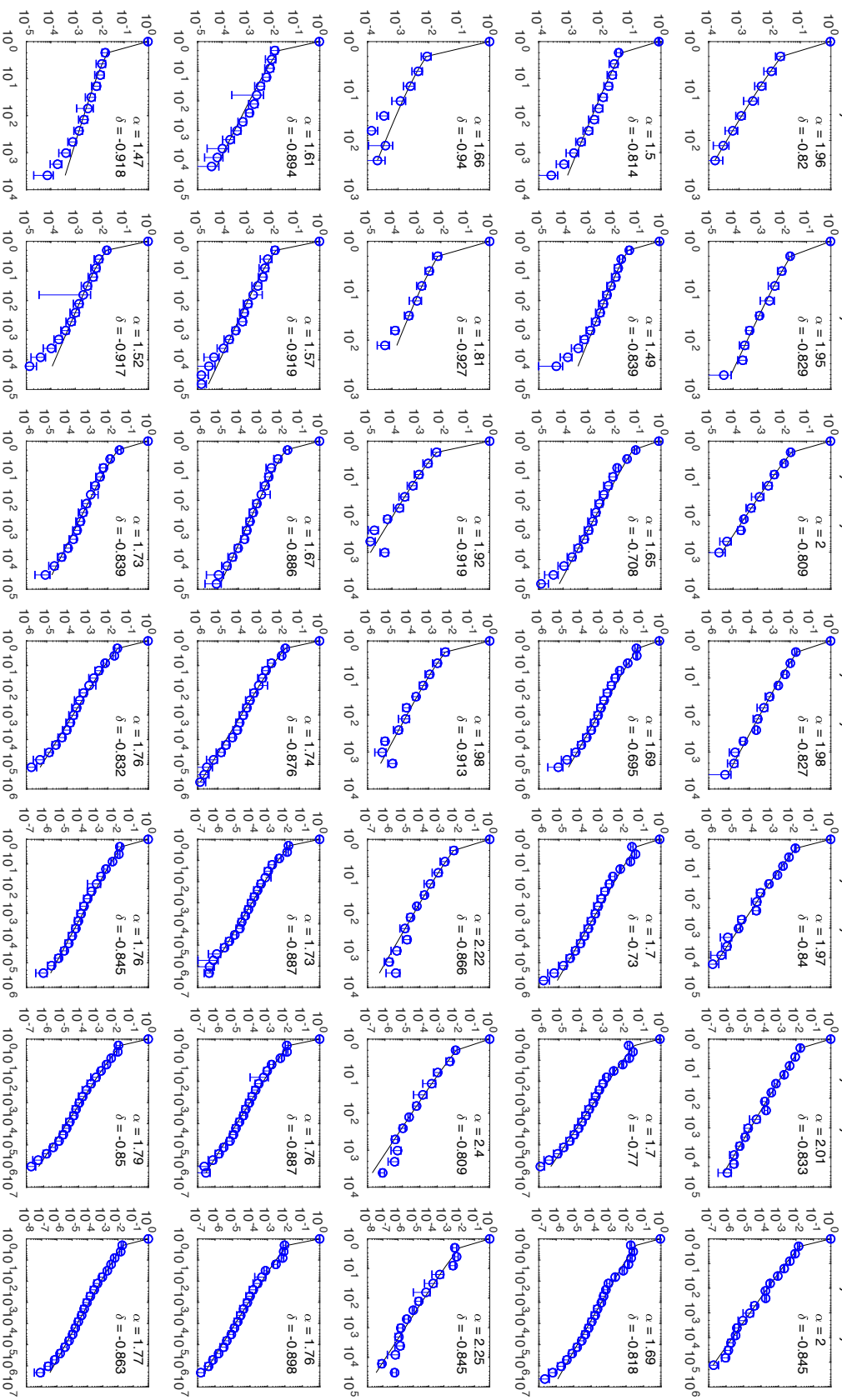
10,000,000

30,000,000

100,000,000

Tokyo 2015 Dec 02-03

## differential cumulative probability



network quantity

source fan-out  
 source packets  
 destination fan-in  
 destination packets  
 link packets

valid packets: 100,000

300,000

1,000,000

3,000,000

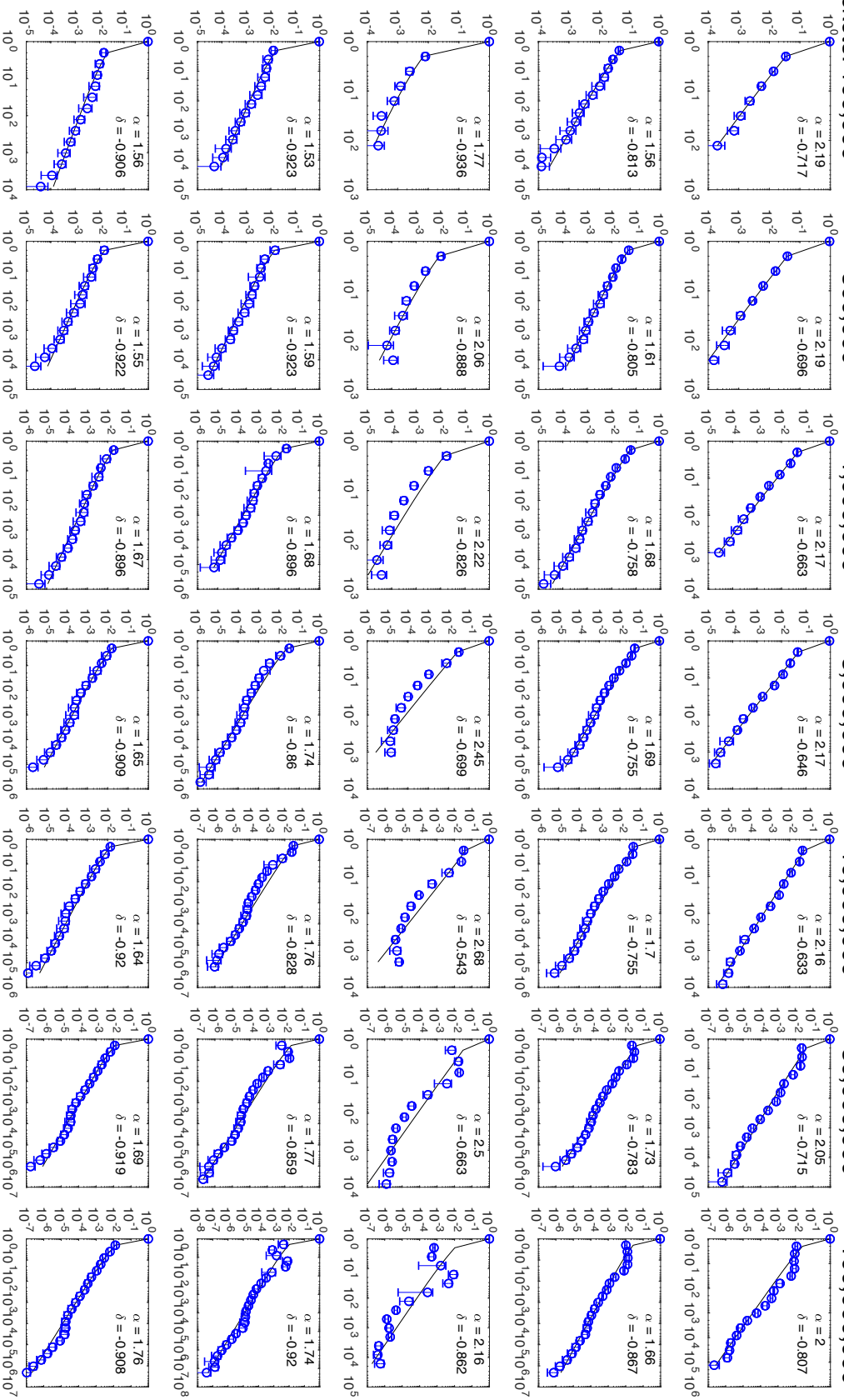
10,000,000

30,000,000

100,000,000

Tokyo 2017 Apr 12-13

differential cumulative probability



network quantity

source fan-out  
source packets  
destination fan-in  
destination packets  
link packets

valid packets: 100,000

300,000

1,000,000

3,000,000

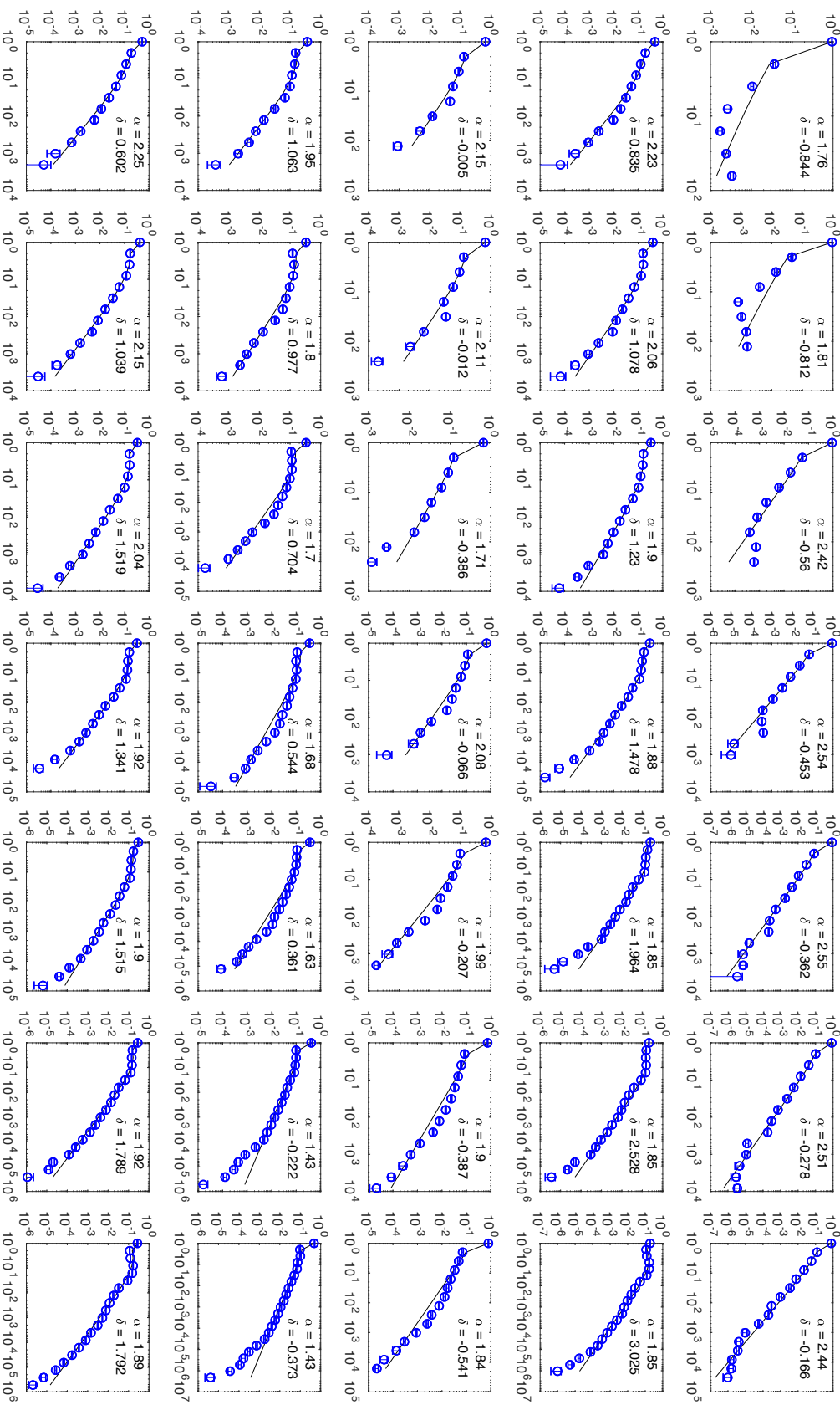
10,000,000

30,000,000

100,000,000

Chicago A 2016 Jan 21

differential cumulative probability



network quantity

source fan-out  
source packets  
destination fan-in  
destination packets  
link packets

valid packets: 100,000

300,000

1,000,000

3,000,000

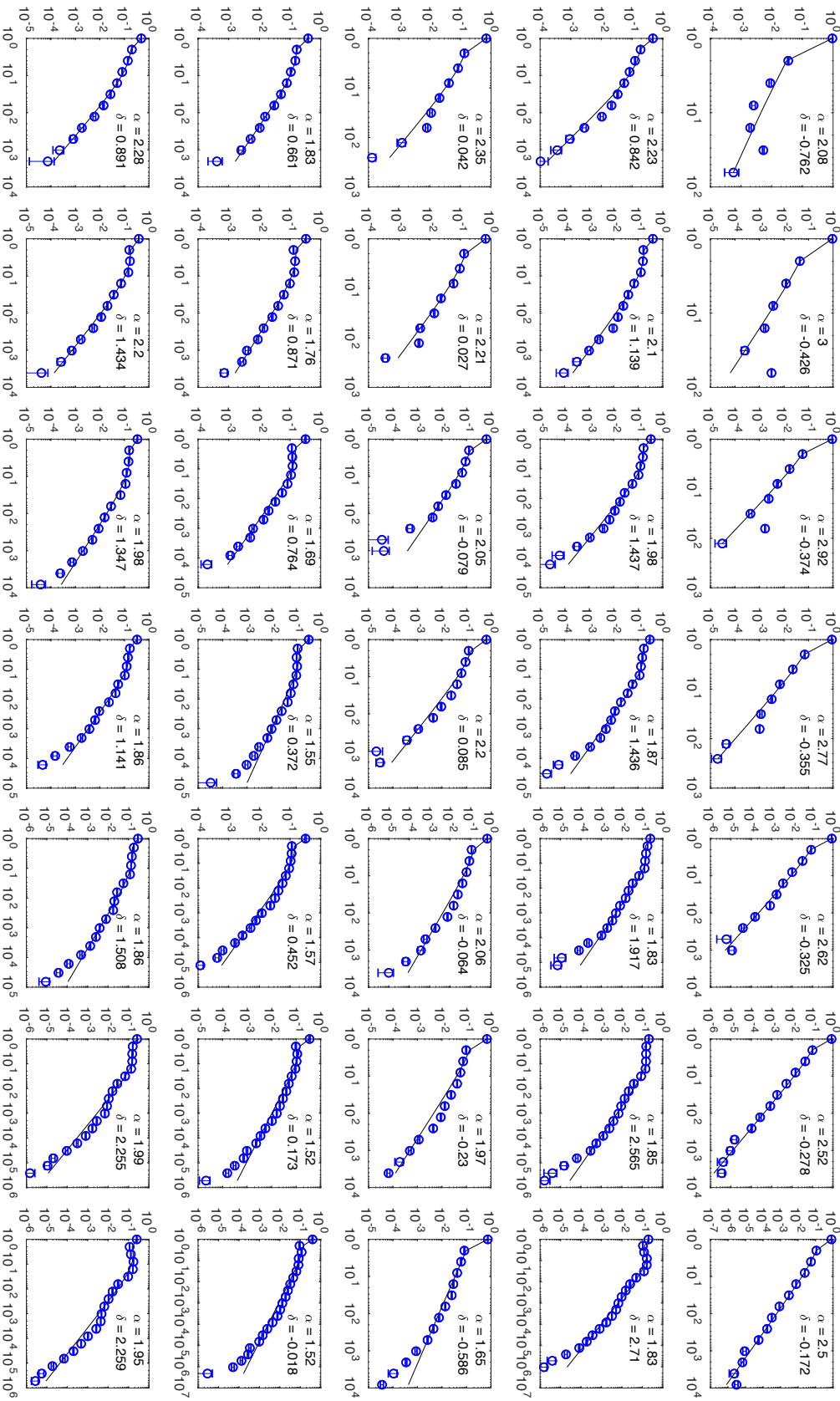
10,000,000

30,000,000

100,000,000

Chicago A 2016 Feb 18

differential cumulative probability



network quantity

source fan-out  
source packets  
destination fan-in  
destination packets  
link packets

valid packets: 100,000

300,000

1,000,000

3,000,000

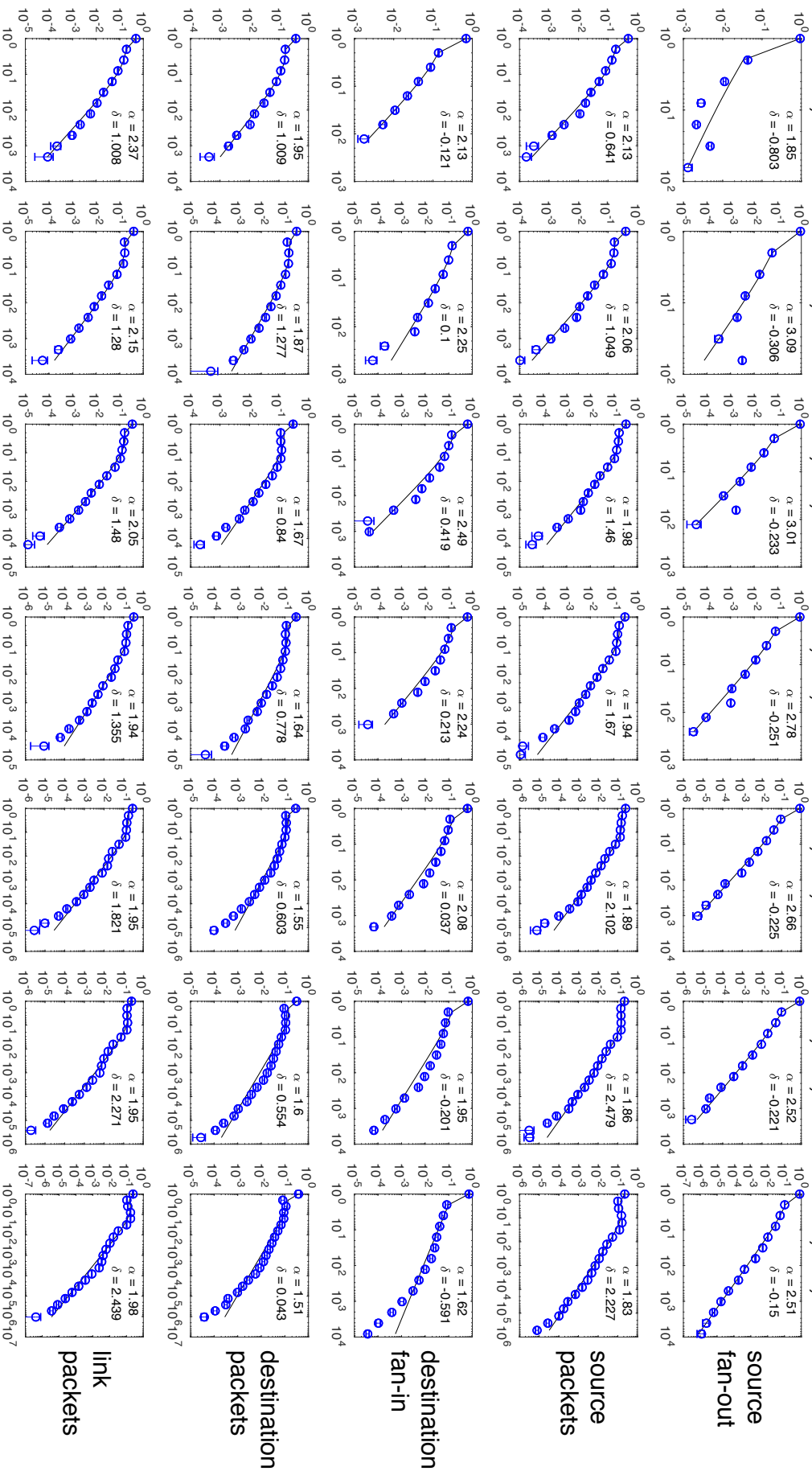
10,000,000

30,000,000

100,000,000

Chicago A 2016 Mar 17

## differential cumulative probability



network quantity

valid packets: 100,000

300,000

1,000,000

3,000,000

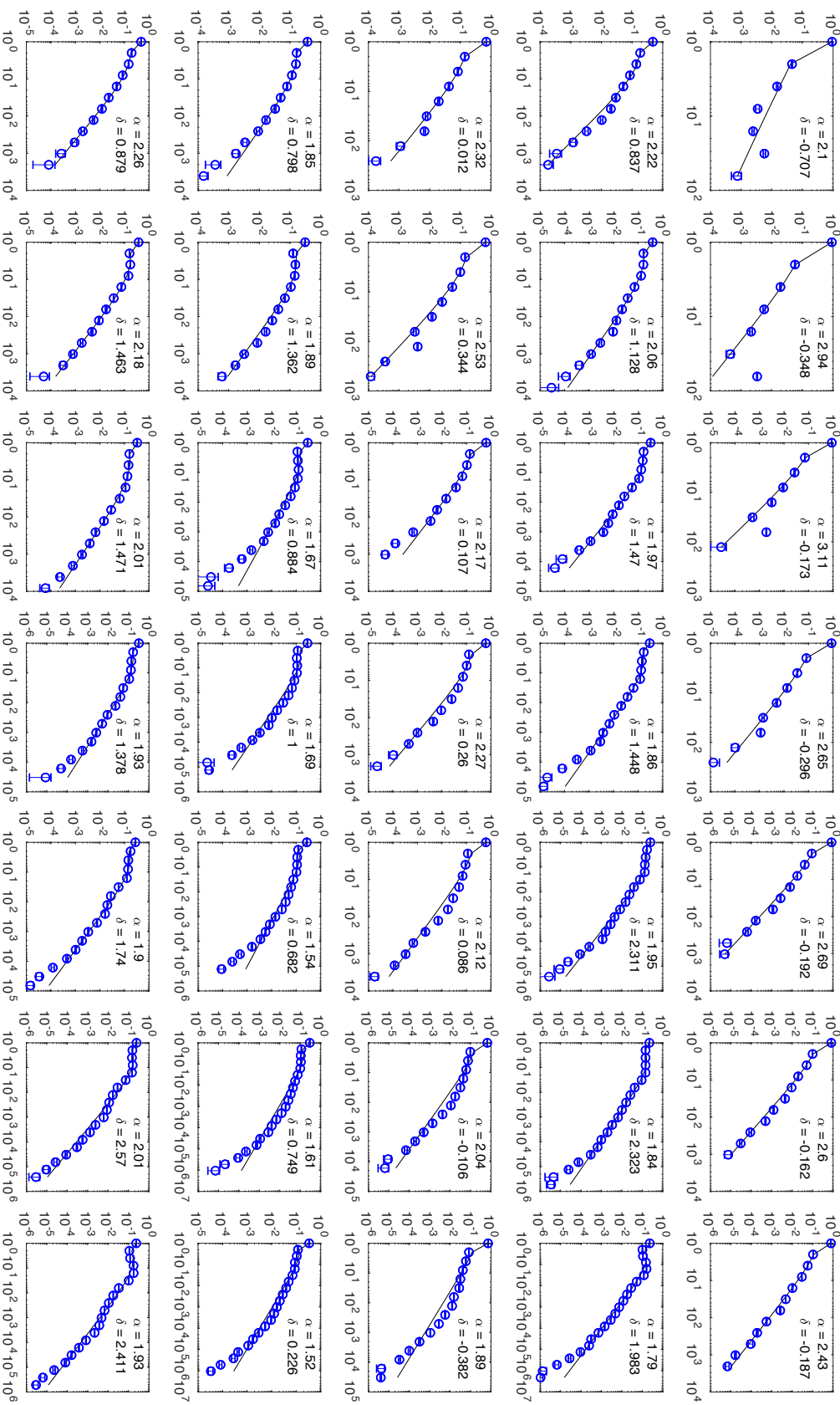
10,000,000

30,000,000

100,000,000

Chicago A 2016 Apr 06

differential cumulative probability



network quantity

source fan-out  
source packets  
destination fan-in  
destination packets  
link packets



valid packets: 100,000

300,000

1,000,000

3,000,000

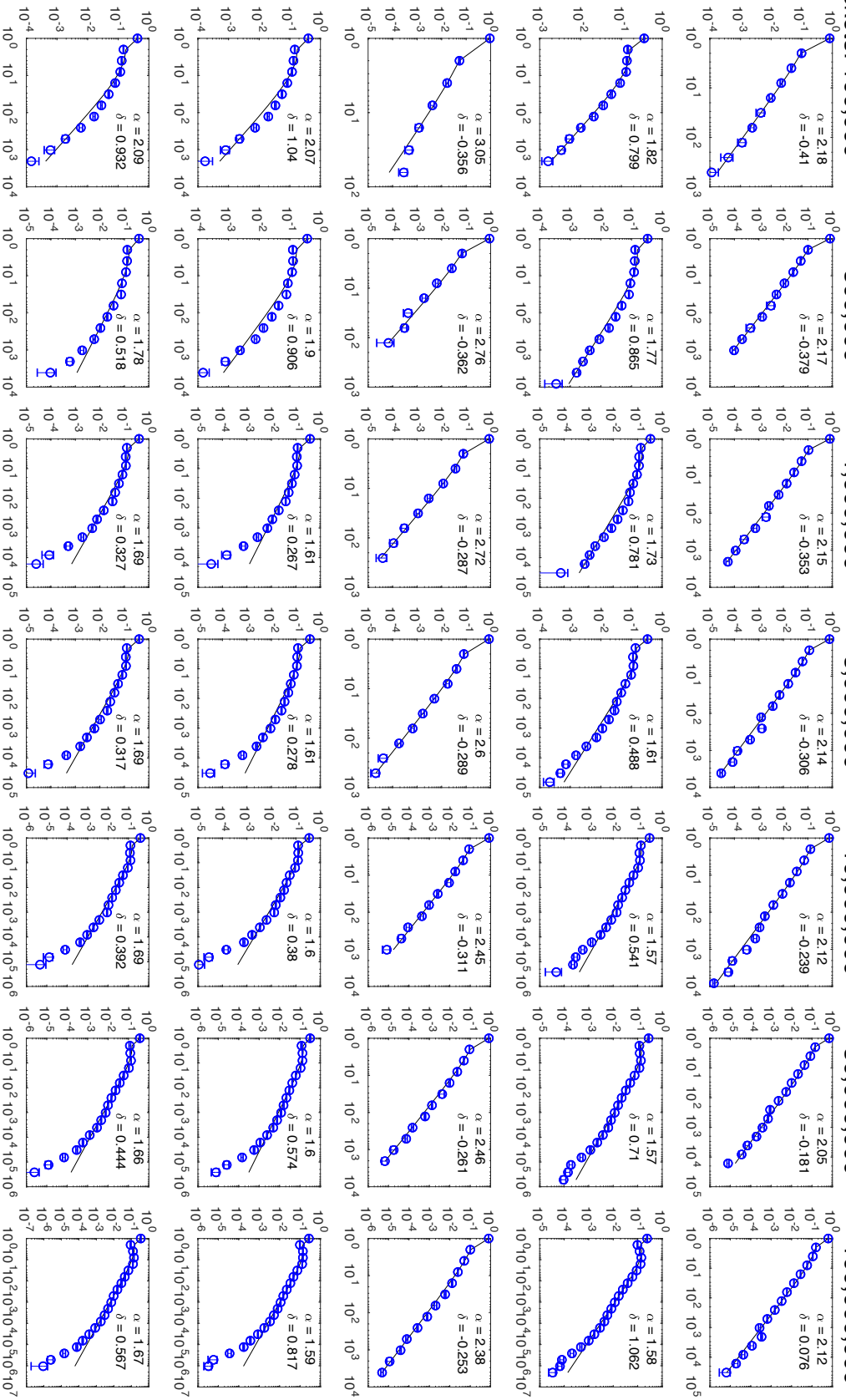
10,000,000

30,000,000

100,000,000

Chicago B 2016 Jan 21

differential cumulative probability



network quantity



valid packets: 100,000

300,000

1,000,000

3,000,000

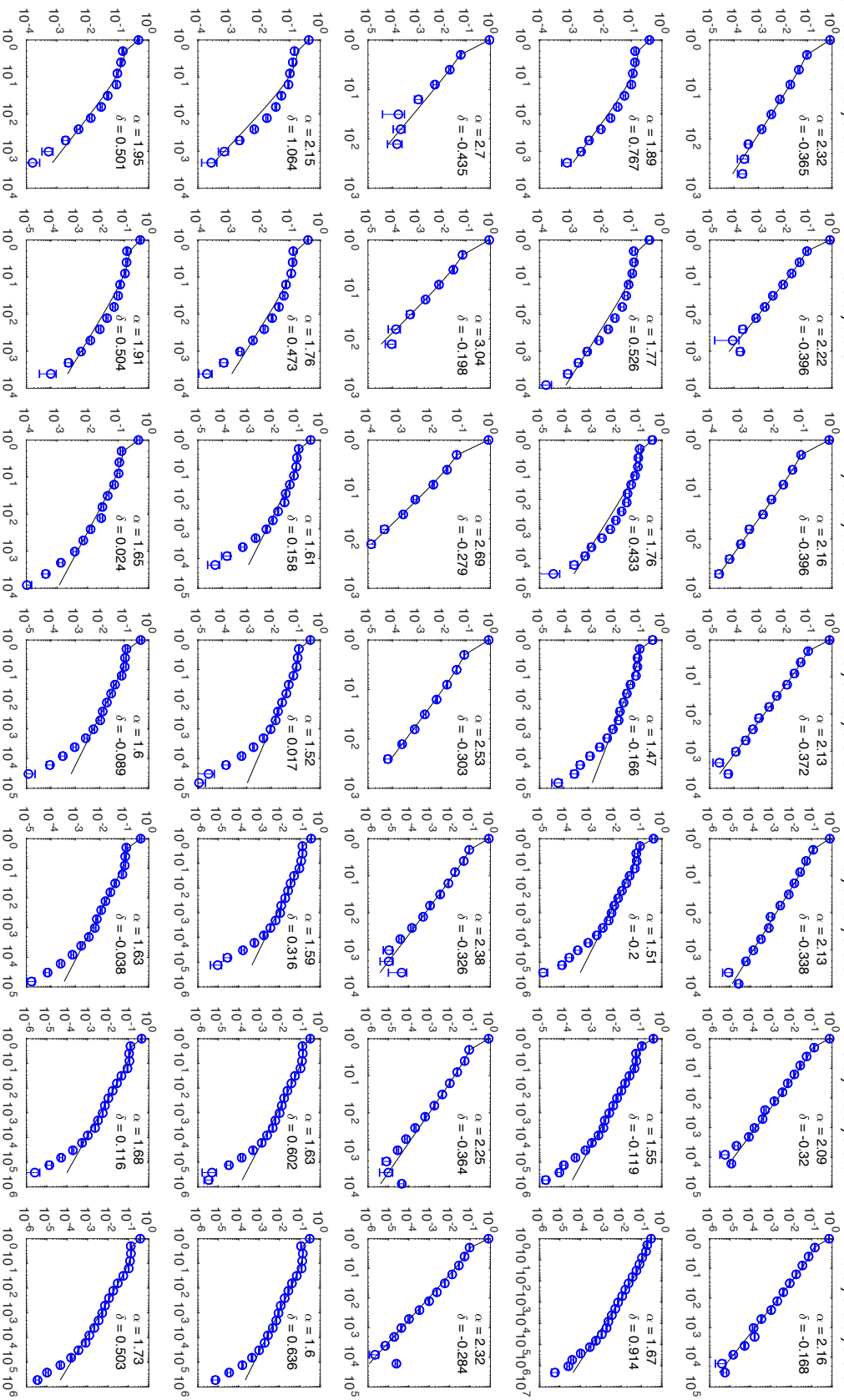
Chicago B 2016 Feb 18

10,000,000

30,000,000

100,000,000

## differential cumulative probability



network quantity



valid packets: 100,000

300,000

1,000,000

3,000,000

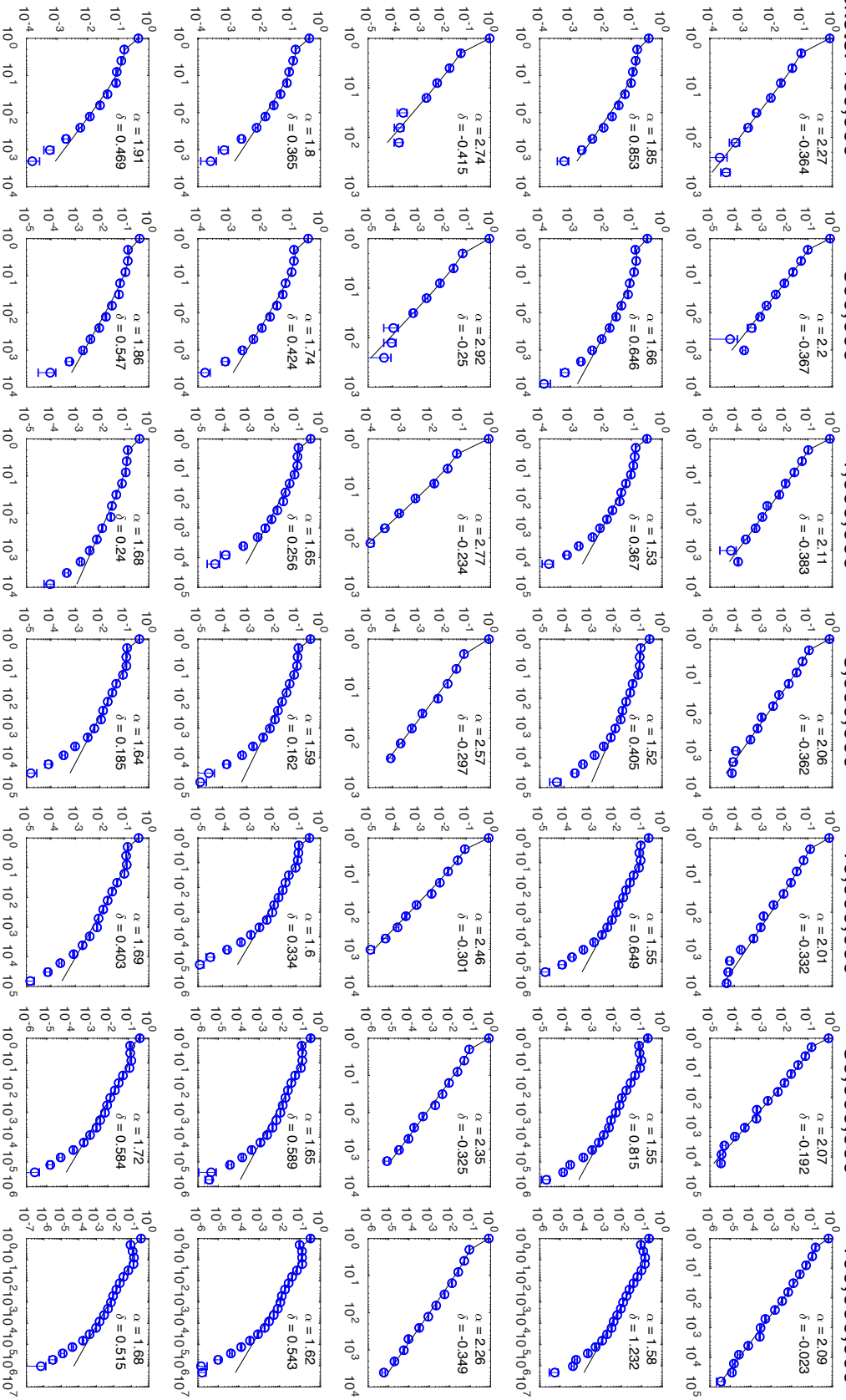
10,000,000

30,000,000

100,000,000

Chicago B 2016 Mar 17

# differential cumulative probability



network quantity

source fan-out  
 source packets  
 destination fan-in  
 destination packets  
 link packets

valid packets: 100,000

300,000

1,000,000

3,000,000

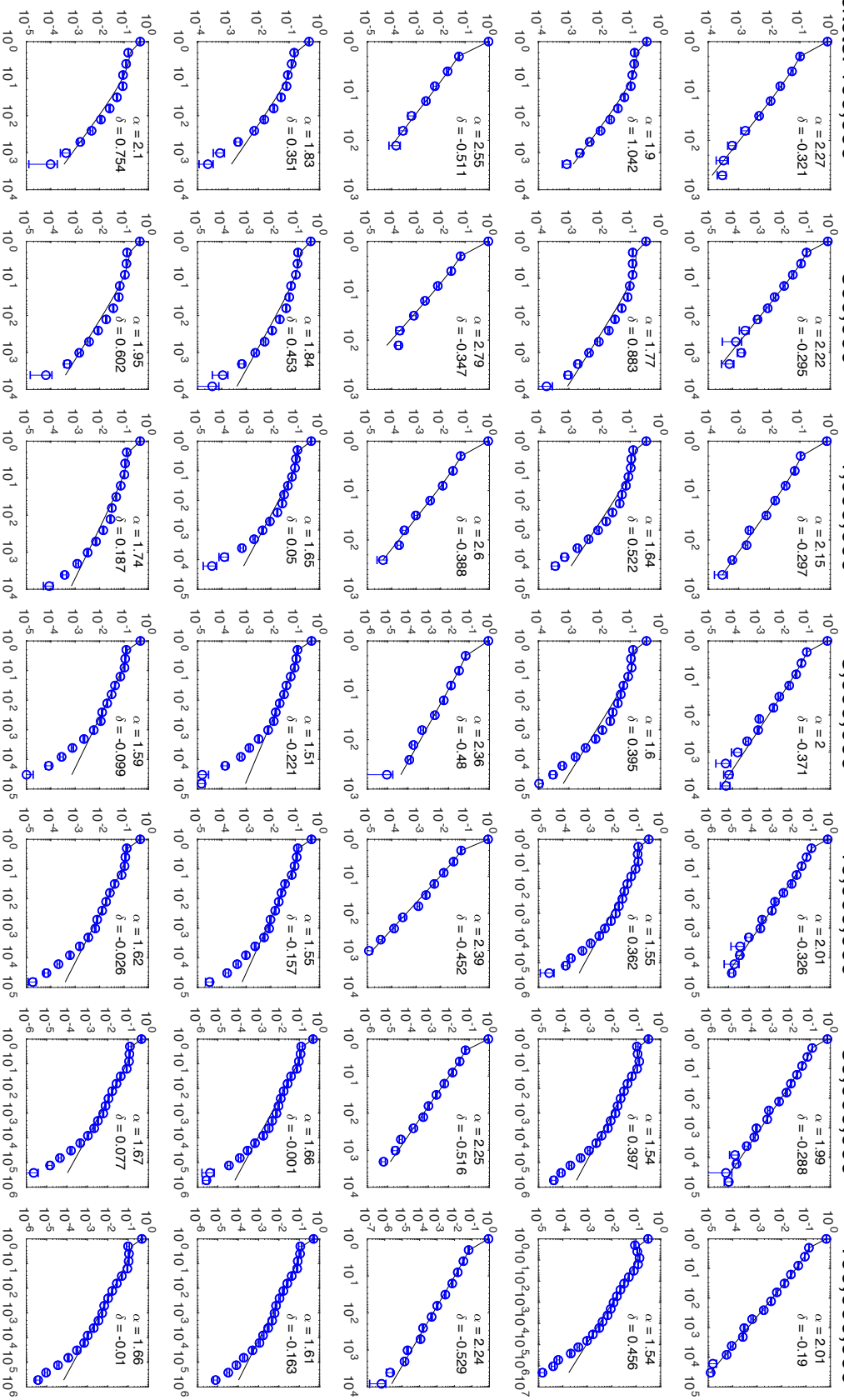
10,000,000

30,000,000

100,000,000

Chicago B 2016 Apr 06

# differential cumulative probability



network quantity

source fan-out  
 source packets  
 destination fan-in  
 destination packets  
 link packets

## S11 Network Topology Measures

Figure 2A depicts the major topological structures in the network traffic. Identification of these topologies and computation of their network statistics can all be obtained from the packet traffic counts aggregated into the sparse matrix  $\mathbf{A}_t$ . Two important network quantities for computing these network topologies are the source fan-out column vector

$$\mathbf{d}_{\text{out}} = |\mathbf{A}_t|_0 \mathbf{1} \quad (\text{S28})$$

and the destination fan-in row vector

$$\mathbf{d}_{\text{in}} = \mathbf{1}^\top |\mathbf{A}_t|_0 \quad (\text{S29})$$

### S11.1 Isolated Links

Isolated links are sources and destinations that each have only one connection. The set of sources that send to only one destination are

$$i_1 = \arg(\mathbf{d}_{\text{out}} = 1) \quad (\text{S30})$$

The set of destinations that receive from only one destination are

$$j_1 = \arg(\mathbf{d}_{\text{in}} = 1) \quad (\text{S31})$$

The isolated links can be found via

$$\mathbf{A}_t(i_1, j_1) \quad (\text{S32})$$

The number of isolated link sources are

$$\mathbf{1}^\top |\mathbf{A}_t(i_1, j_1)|_0 \quad (\text{S33})$$

The number of packets traversing isolated links is given by

$$\mathbf{1}^\top \mathbf{A}_t(i_1, j_1) \mathbf{1} \quad (\text{S34})$$

The number of unique isolated links can be computed from

$$\mathbf{1}^\top |\mathbf{A}_t(i_1, j_1)|_0 \mathbf{1} \quad (\text{S35})$$

The number of isolated link destinations are

$$|\mathbf{1}^\top \mathbf{A}_t(i_1, j_1)|_0 \mathbf{1} \quad (\text{S36})$$

By definition, the number of isolated sources, the number of isolated links, and the number of isolated destinations are all the same value.

## S11.2 Supernodes

The first, second, third, ... supernode is the source or destination with the first, second, third, ... most links. The identity of the first supernode is given by

$$k_{\max} = \operatorname{argmax}(\mathbf{d}_{\text{out}} + \mathbf{d}_{\text{in}}) \quad (\text{S37})$$

The leaves of a supernode are those sources and destinations whose only connection is to the supernode. The supernode source leaves can be found via

$$\mathbf{A}_t(i_1, k_{\max}) \quad (\text{S38})$$

The supernode destination leaves can be found via

$$\mathbf{A}_t(k_{\max}, j_1) \quad (\text{S39})$$

The number of supernode leaf sources are

$$\mathbf{1}^\top |\mathbf{A}_t(i_1, k_{\max}) \mathbf{1}|_0 \quad (\text{S40})$$

The number of packets traversing supernode leaves is given by

$$\mathbf{1}^\top \mathbf{A}_t(i_1, k_{\max}) + \mathbf{A}_t(k_{\max}, j_1) \mathbf{1} \quad (\text{S41})$$

The number of unique supernode leaf links can be computed from

$$\mathbf{1}^\top |\mathbf{A}_t(i_1, k_{\max})|_0 + |\mathbf{A}_t(k_{\max}, j_1)|_0 \mathbf{1} \quad (\text{S42})$$

The number of supernode leaf destinations are

$$|\mathbf{1}^\top \mathbf{A}_t(k_{\max}, j_1)|_0 \mathbf{1} \quad (\text{S43})$$

Subsequent supernodes can be computed by eliminating the prior supernode and repeating the above calculations.

### S11.3 Core

The core of a network can be defined in a variety of ways. In this work, the network core is meant to convey the concept of a collection of sources and destinations that are not isolated and are multiply connected. The core is defined as the collection of sources and destinations whereby every source and destination has more than one connection. In this context, the core does not include the first five supernodes although only the first supernode is significant, and whether or not the other supernodes are included has minimal impact on the core calculations for these data. The set of sources that send to more than one destination, excluding the supernode(s), is

$$i_{\text{core}} = \arg(1 < \mathbf{d}_{\text{out}} < \mathbf{d}_{\text{out}}(k_{\max})) \quad (\text{S44})$$

The set of destinations that receive from more than one source, excluding the supernode(s), is

$$j_{\text{core}} = \arg(1 < \mathbf{d}_{\text{in}} < \mathbf{d}_{\text{in}}(k_{\max})) \quad (\text{S45})$$

The core links can be found via

$$\mathbf{A}_t(i_{\text{core}}, j_{\text{core}}) \quad (\text{S46})$$

The number of core sources is

$$\mathbf{1}^\top |\mathbf{A}_t(i_{\text{core}}, j_{\text{core}})|_0 \mathbf{1} \quad (\text{S47})$$

The number of core packets is given by

$$\mathbf{1}^\top \mathbf{A}_t(i_{\text{core}}, j_{\text{core}}) \mathbf{1} \quad (\text{S48})$$

The number of unique core links can be computed from

$$\mathbf{1}^\top |\mathbf{A}_t(i_{\text{core}}, j_{\text{core}})|_0 \mathbf{1} \quad (\text{S49})$$

The number of core destinations is

$$|\mathbf{1}^\top \mathbf{A}_t(i_{\text{core}}, j_{\text{core}})|_0 \mathbf{1} \quad (\text{S50})$$

## S11.4 Core Leaves

The core leaves are sources and destinations that have one connection to a core source or destination. The core source leaves can be found via

$$\mathbf{A}_t(i_1, k_{\text{core}}) \quad (\text{S51})$$

The core destination leaves can be found via

$$\mathbf{A}_t(k_{\text{core}}, j_1) \quad (\text{S52})$$

The number of core leaf sources is

$$\mathbf{1}^\top |\mathbf{A}_t(i_1, k_{\text{core}})|_0 \mathbf{1} \quad (\text{S53})$$

The number of core leaf packets is given by

$$\mathbf{1}^\top \mathbf{A}_t(i_1, k_{\text{core}}) + \mathbf{A}_t(k_{\text{core}}, j_1) \mathbf{1} \quad (\text{S54})$$

The number of unique core leaf links can be computed from

$$\mathbf{1}^\top |\mathbf{A}_t(i_1, k_{\text{core}})|_0 + |\mathbf{A}_t(k_{\text{core}}, j_1)|_0 \mathbf{1} \quad (\text{S55})$$

The number of core leaf destinations is

$$|\mathbf{1}^\top \mathbf{A}_t(k_{\text{core}}, j_1)|_0 \mathbf{1} \quad (\text{S56})$$

## S12 Measured Packet Fractions in Different Topologies

Figure S6A-D shows the fraction of the sources, links, total packets, and destinations in each of the measured topologies for the all the locations.

Figure S6: **Fraction of data in different network topologies.** Internet traffic forms networks consisting of a variety of topologies: isolated links, supernode leaves connected to a supernode, densely connected core(s) with corresponding core leaves. Horizontal and vertical axis are the corresponding fraction of the sources, links, total packets and destinations that are in various topologies for each location, time, and seven packet windows ( $N_V = 10^5, \dots, 10^8$ ). Plot label is the type of data in each plot: sources, links, total packets, and destinations.

(A) Fraction of data in isolated links, core leaves, and supernode leaves versus the fraction of data in the core.

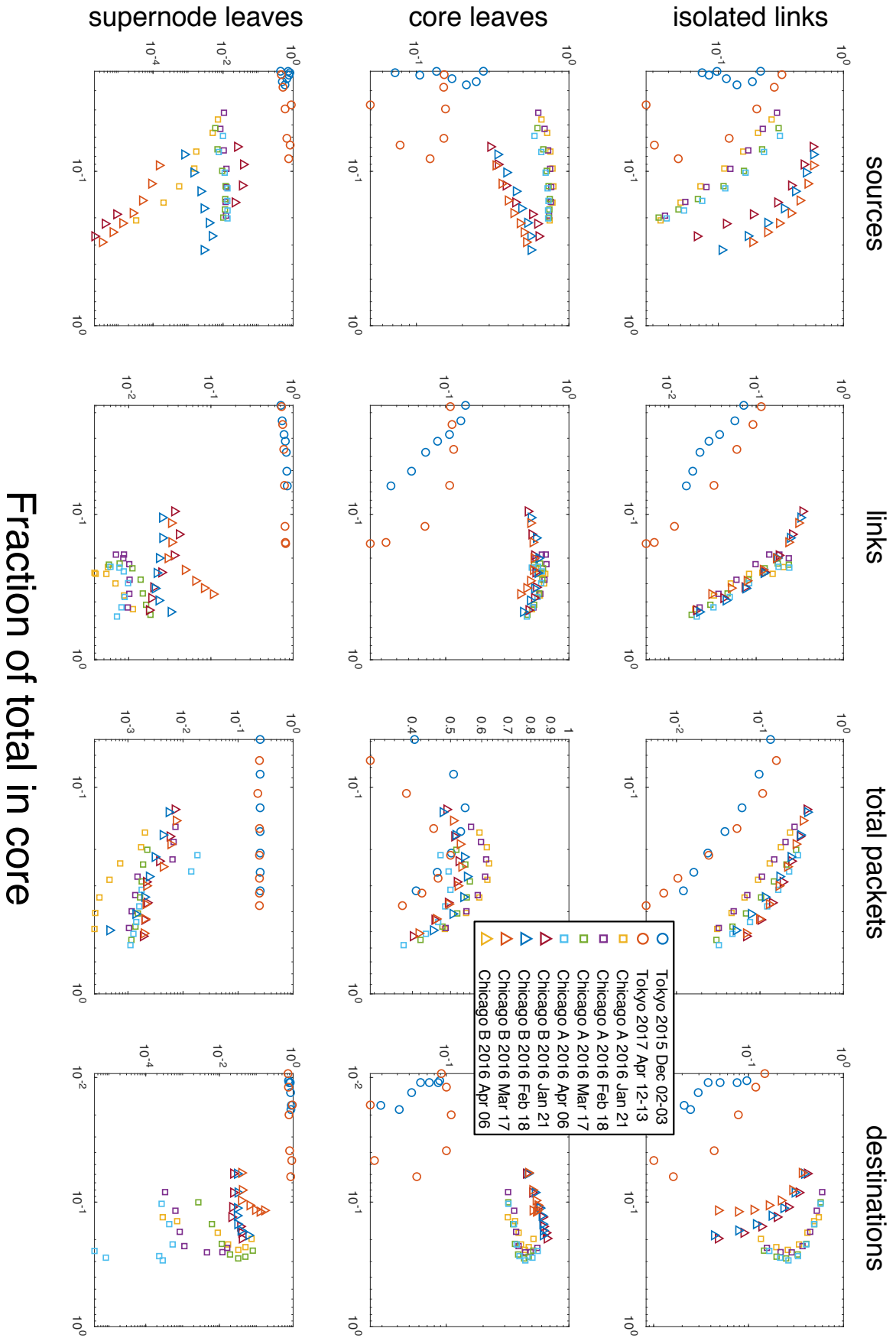
(B) Fraction of data in the core, core leaves, and supernode leaves versus the fraction of data in isolated links.

(C) Fraction of data in the core, isolated links, and supernode leaves versus the fraction of data in core leaves.

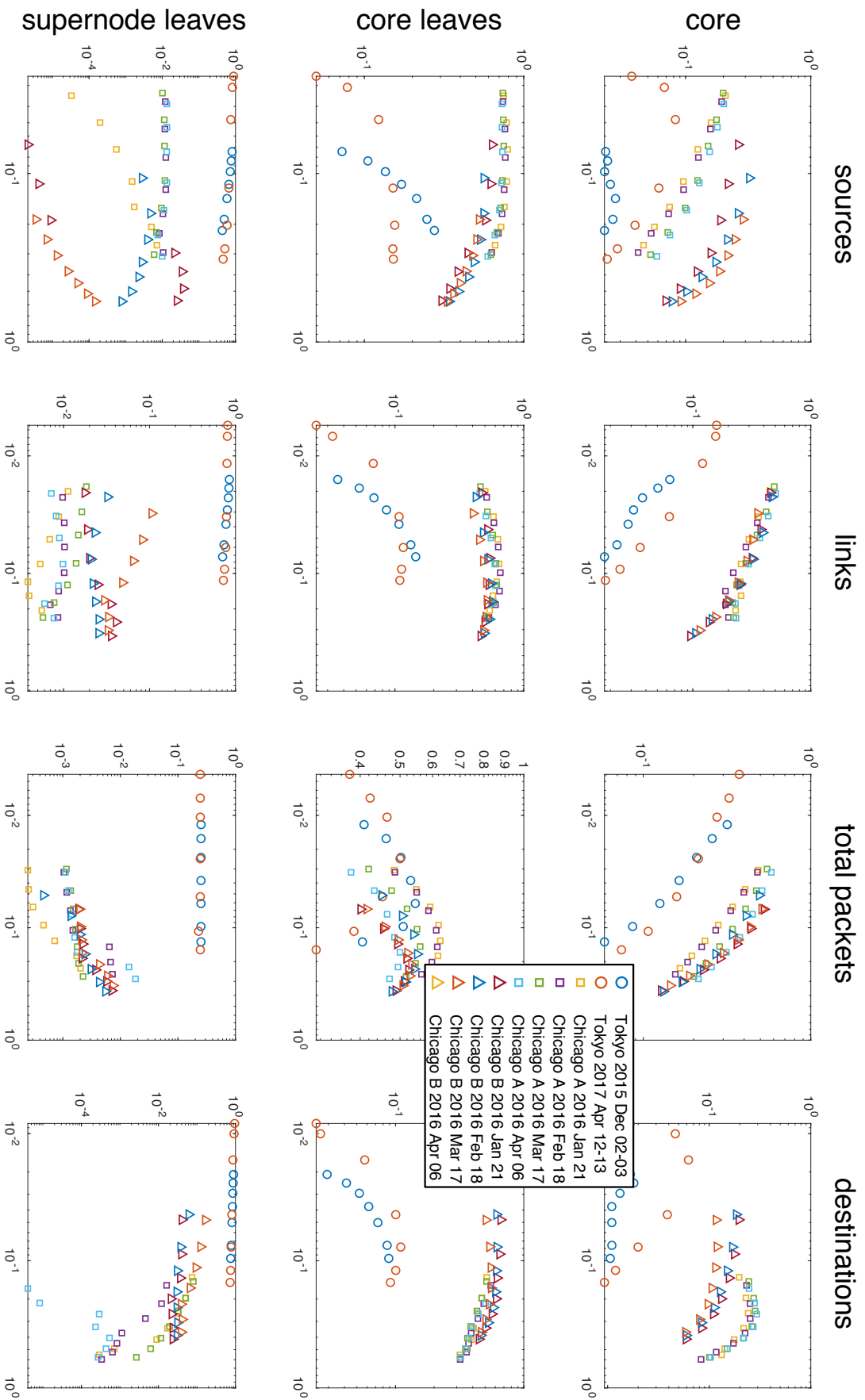
(D) Fraction of data in the core, isolated links, and core leaves versus the fraction of data in supernode leaves.



Fraction of total in:



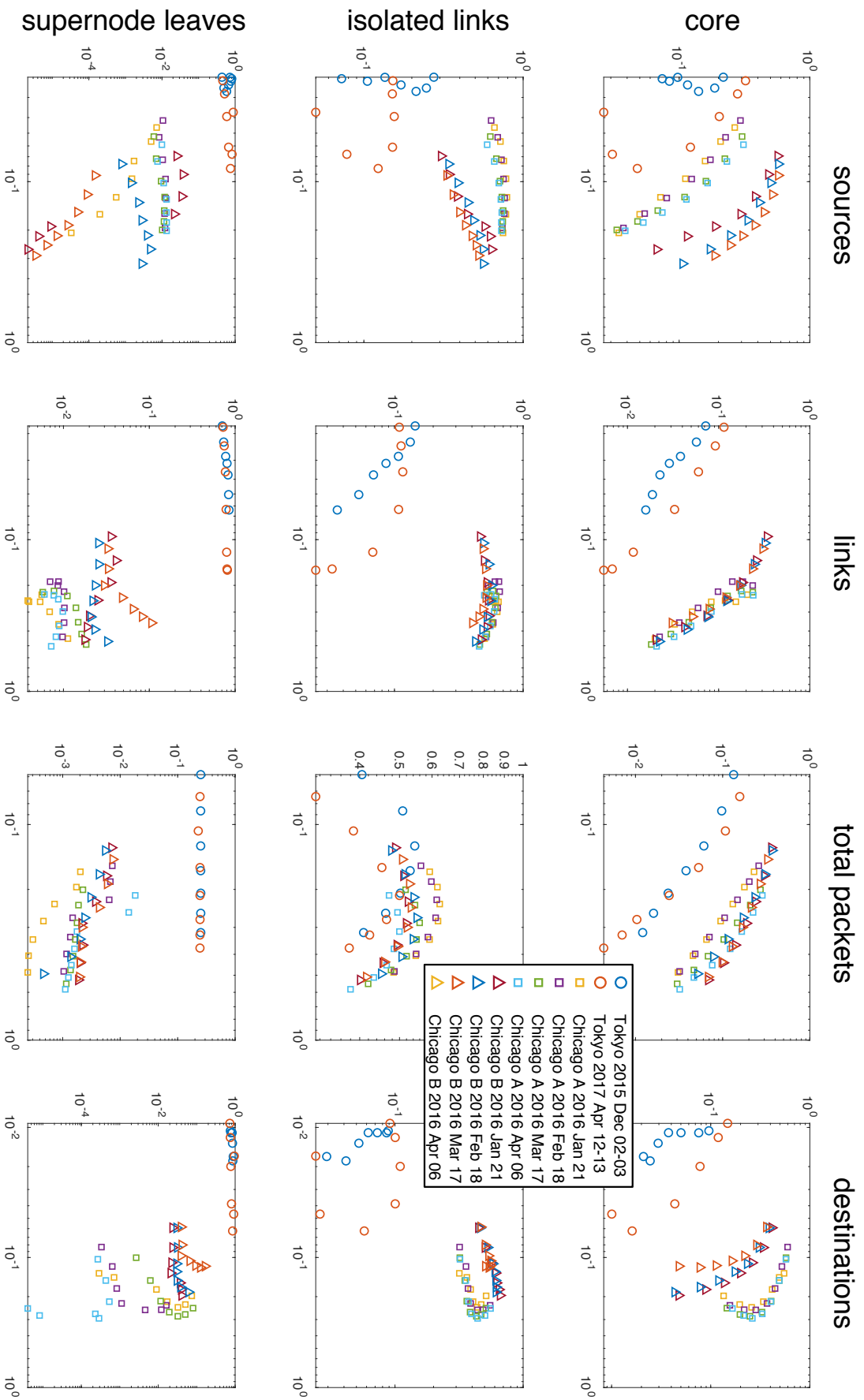
# Fraction of total in:



Fraction of total in isolated links

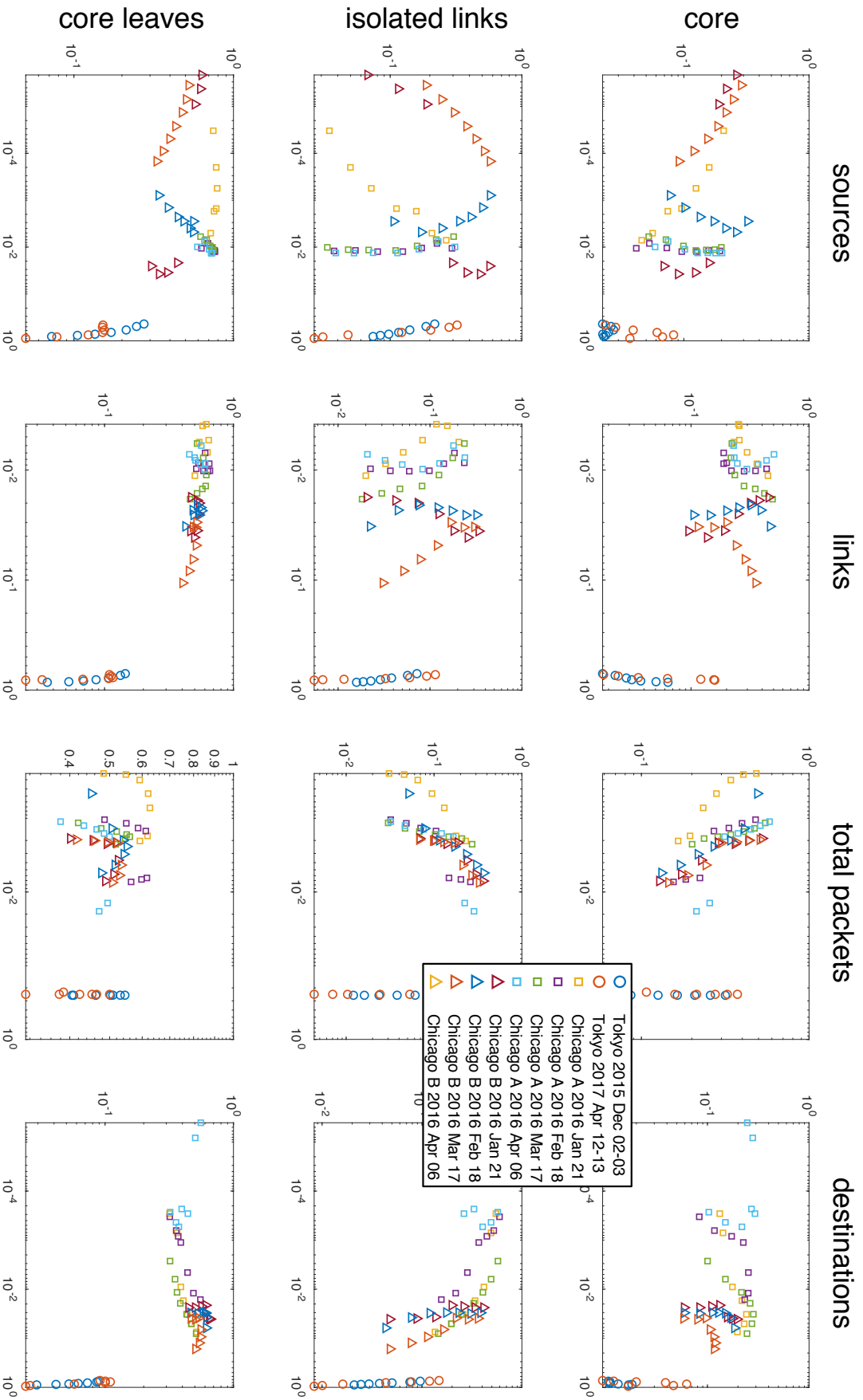


# Fraction of total in:



Fraction of total in core leaves

Fraction of total in:



Fraction of total in supernode leaves

## S13 Topology and the Model Leaf Parameter

Internet traffic forms networks consisting of a variety of topologies: isolated links, supernode leaves connected to a supernode, densely connected core(s) with corresponding core leaves. In many cases the network topology is highly correlated with the modified Zipf-Mandelbrot model leaf parameter  $1/(1 + \delta)^\alpha$ , which corresponds to the relative importance of  $p(d = 1)$ . Figure S7A-E shows the fraction of the sources, links, total packets, and destinations in each of the measured topologies for the all the locations as a function of the modified Zipf-Mandelbrot leaf parameter computed from the model fits of the source packets, source fan-out, link packets, destination fan-in, and destination packets taken from Figure S5A-J.

Figure S7: **Topology versus modified Zipf-Mandelbrot model leaf parameter.** Vertical axis are the corresponding fraction of the sources, links, total packets and destinations that are in various topologies. Horizontal axis is the value of the model parameter taken from the source packet, source fan-out, link packet, destination fan-in and destination packet fits for each location, time, and seven packet windows ( $N_V = 10^5, \dots, 10^8$ ). Plot label is the type of data in each plot: sources, links, total packets, and destinations.

(A) Fraction of data in the core, isolated links, core leaves, and supernode leaves versus the model leaf parameter computed from the source packet modified Zipf-Mandelbrot model fits.

(B) Fraction of data in the core, isolated links, core leaves, and supernode leaves versus the model leaf parameter computed from the source fan-out modified Zipf-Mandelbrot model fits.

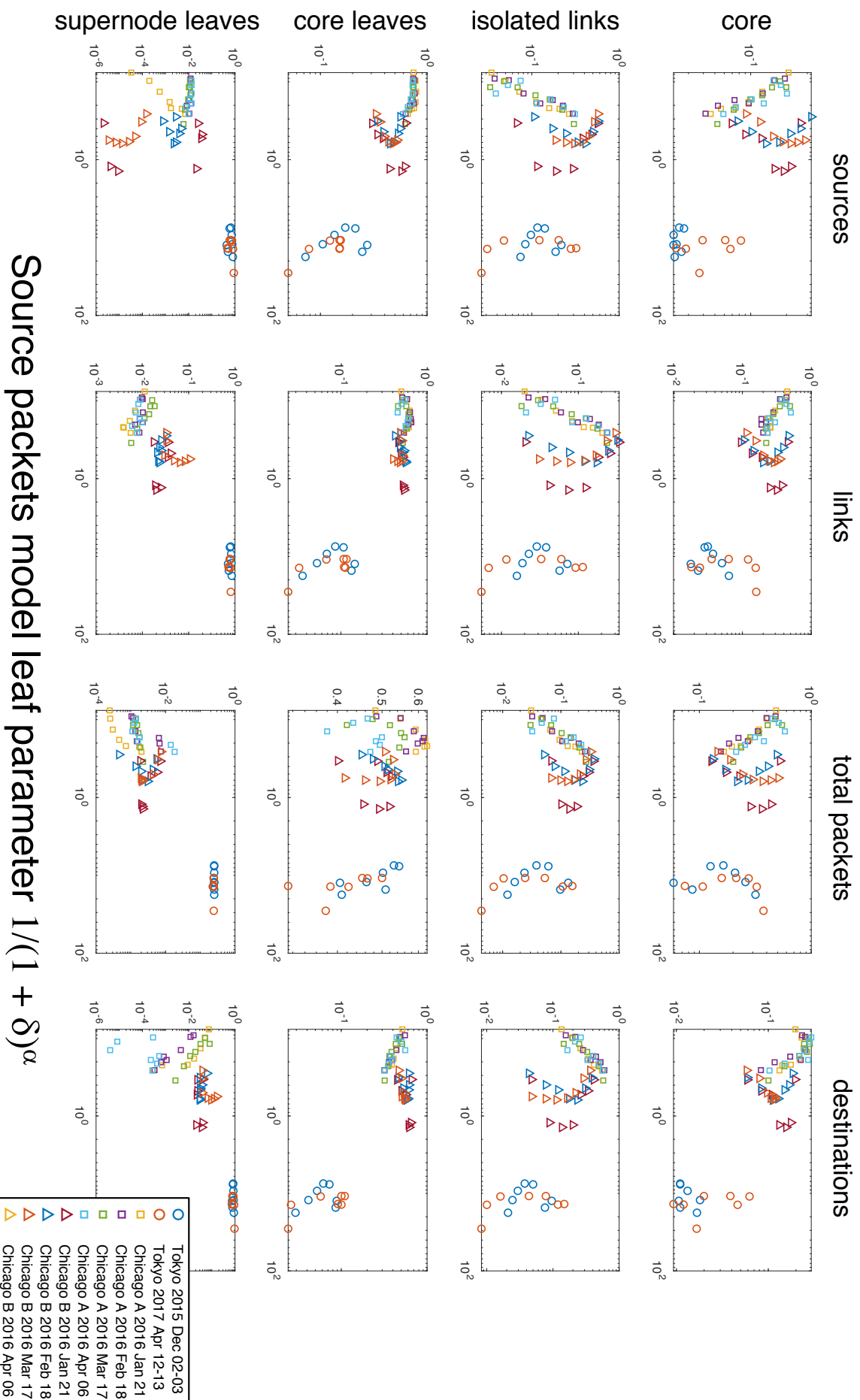
(C) Fraction of data in the core, isolated links, core leaves, and supernode leaves versus the model leaf parameter computed from the link packets modified Zipf-Mandelbrot model fits.

(D) Fraction of data in the core, isolated links, core leaves, and supernode leaves versus the model leaf parameter computed from the destination fan-out modified Zipf-Mandelbrot model fits.

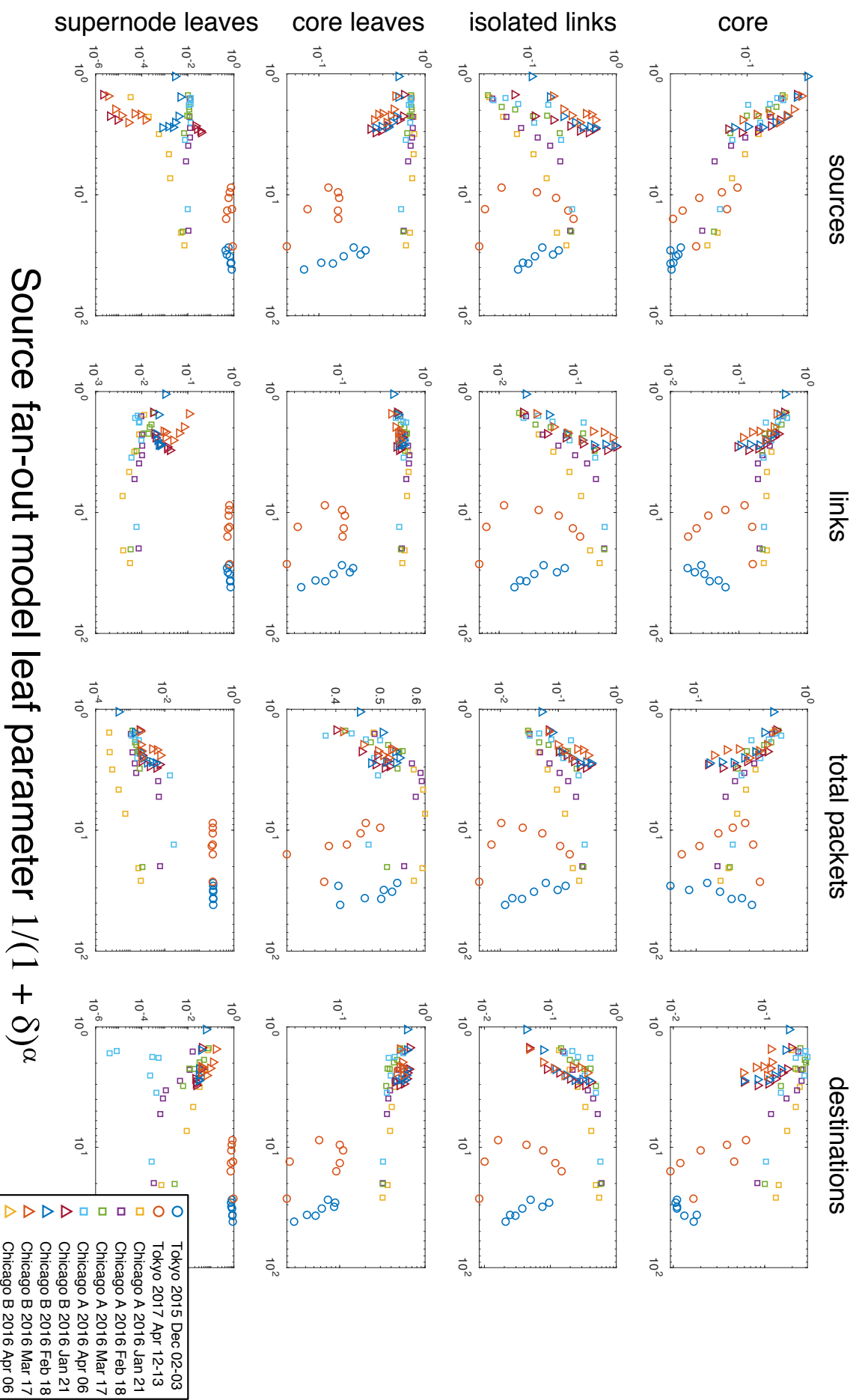
(E) Fraction of data in the core, isolated links, core leaves, and supernode leaves versus the model leaf parameter computed from the destination packets modified Zipf-Mandelbrot model fits.

**A**

Fraction of total in:

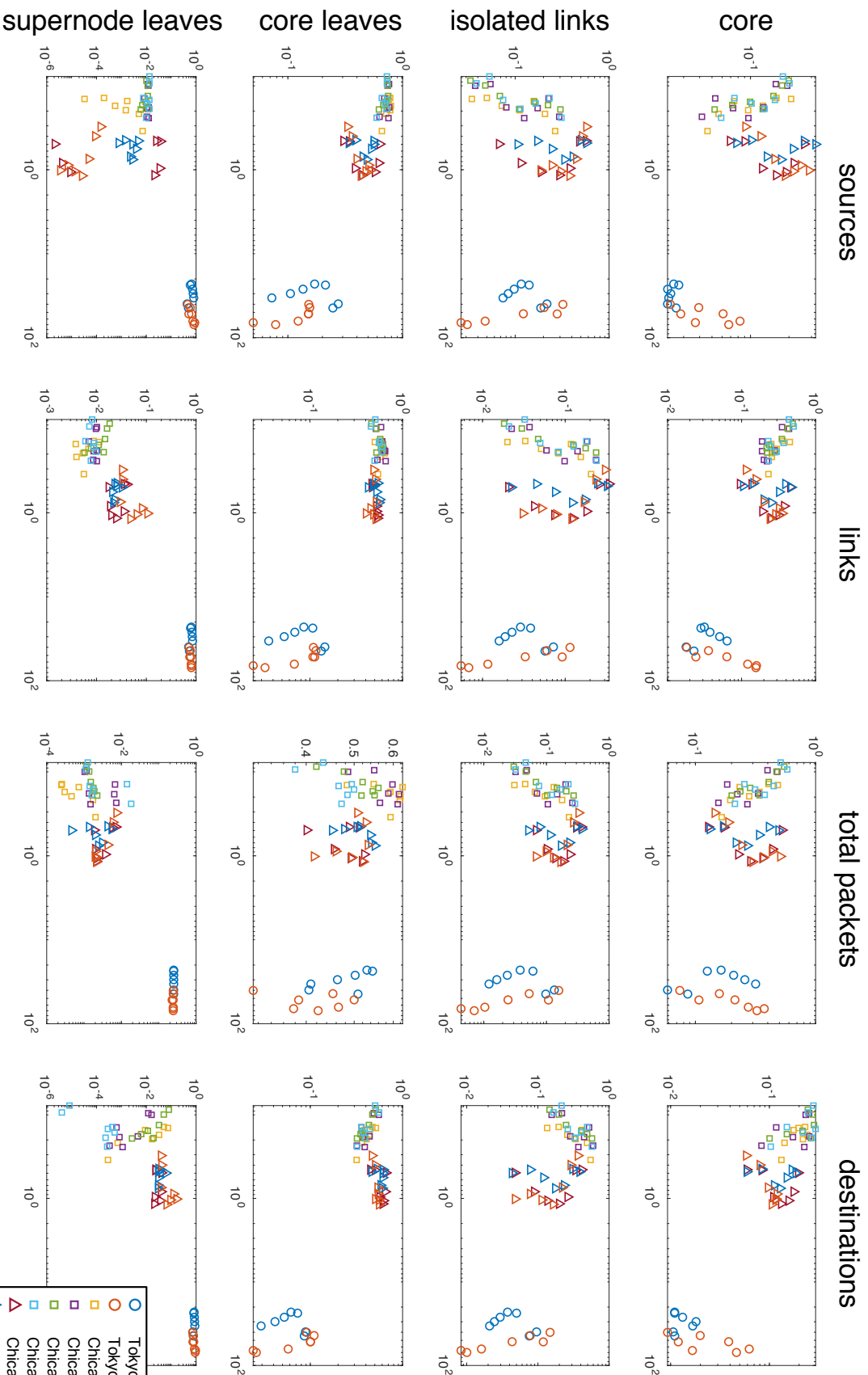


Fraction of total in:



**C**

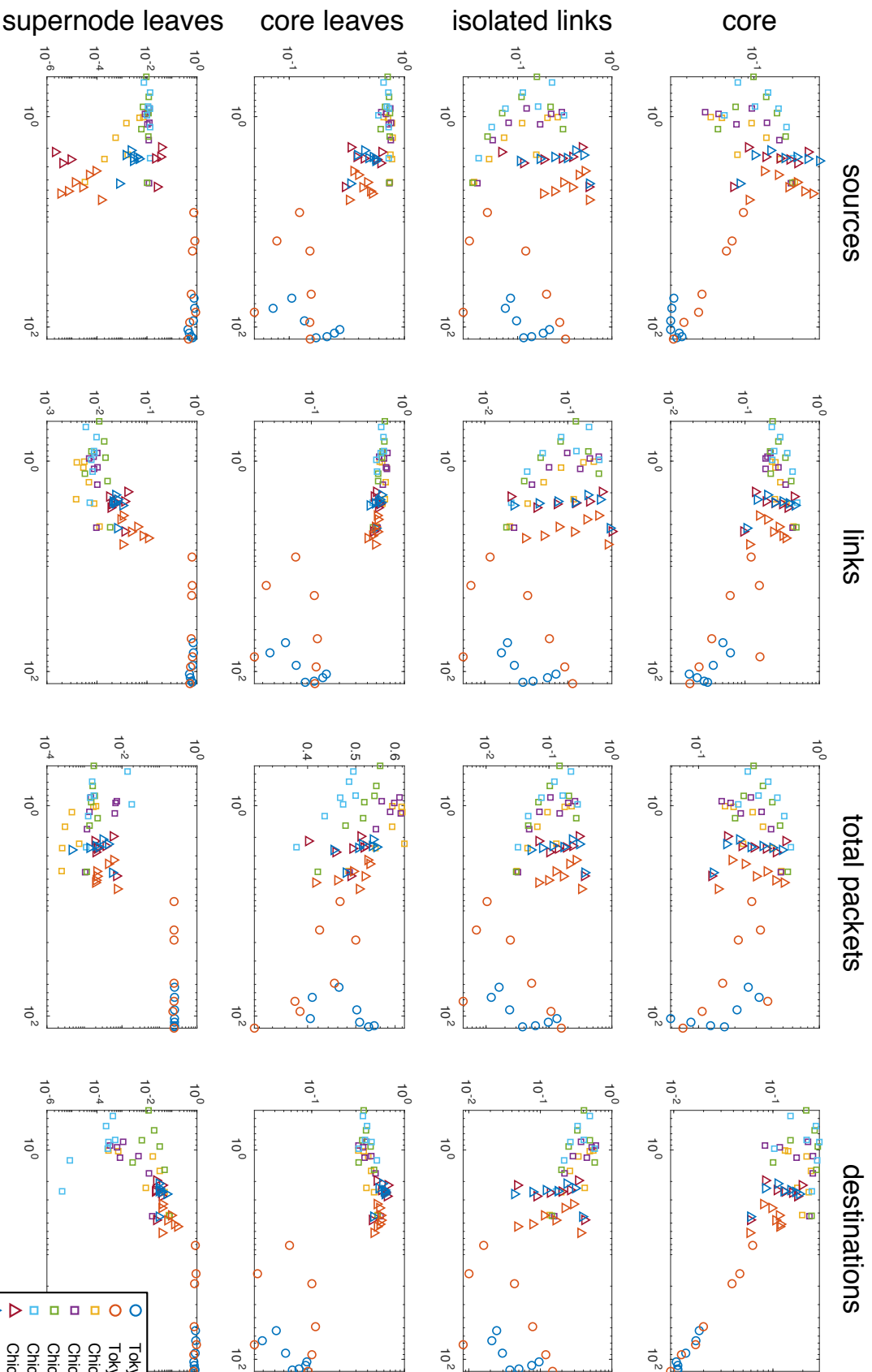
Fraction of total in:

Link packets model leaf parameter  $1/(1 + \delta)^\alpha$ 

- Tokyo 2015 Dec 02-03
- Tokyo 2017 Apr 12-13
- Chicago A 2016 Jan 21
- Chicago A 2016 Feb 18
- Chicago A 2016 Mar 17
- Chicago A 2016 Apr 06
- Chicago B 2016 Jan 21
- Chicago B 2016 Feb 18
- Chicago B 2016 Mar 17
- Chicago B 2016 Apr 06
- Tokyo 2015 Dec 02-03
- Tokyo 2017 Apr 12-13
- Chicago A 2016 Jan 21
- Chicago A 2016 Feb 18
- Chicago A 2016 Mar 17
- Chicago A 2016 Apr 06
- Chicago B 2016 Jan 21
- Chicago B 2016 Feb 18
- Chicago B 2016 Mar 17
- Chicago B 2016 Apr 06
- △ Tokyo 2015 Dec 02-03
- △ Tokyo 2017 Apr 12-13
- △ Chicago A 2016 Jan 21
- △ Chicago A 2016 Feb 18
- △ Chicago A 2016 Mar 17
- △ Chicago A 2016 Apr 06
- △ Chicago B 2016 Jan 21
- △ Chicago B 2016 Feb 18
- △ Chicago B 2016 Mar 17
- △ Chicago B 2016 Apr 06
- ▽ Tokyo 2015 Dec 02-03
- ▽ Tokyo 2017 Apr 12-13
- ▽ Chicago A 2016 Jan 21
- ▽ Chicago A 2016 Feb 18
- ▽ Chicago A 2016 Mar 17
- ▽ Chicago A 2016 Apr 06
- ▽ Chicago B 2016 Jan 21
- ▽ Chicago B 2016 Feb 18
- ▽ Chicago B 2016 Mar 17
- ▽ Chicago B 2016 Apr 06
- ◇ Tokyo 2015 Dec 02-03
- ◇ Tokyo 2017 Apr 12-13
- ◇ Chicago A 2016 Jan 21
- ◇ Chicago A 2016 Feb 18
- ◇ Chicago A 2016 Mar 17
- ◇ Chicago A 2016 Apr 06
- ◇ Chicago B 2016 Jan 21
- ◇ Chicago B 2016 Feb 18
- ◇ Chicago B 2016 Mar 17
- ◇ Chicago B 2016 Apr 06



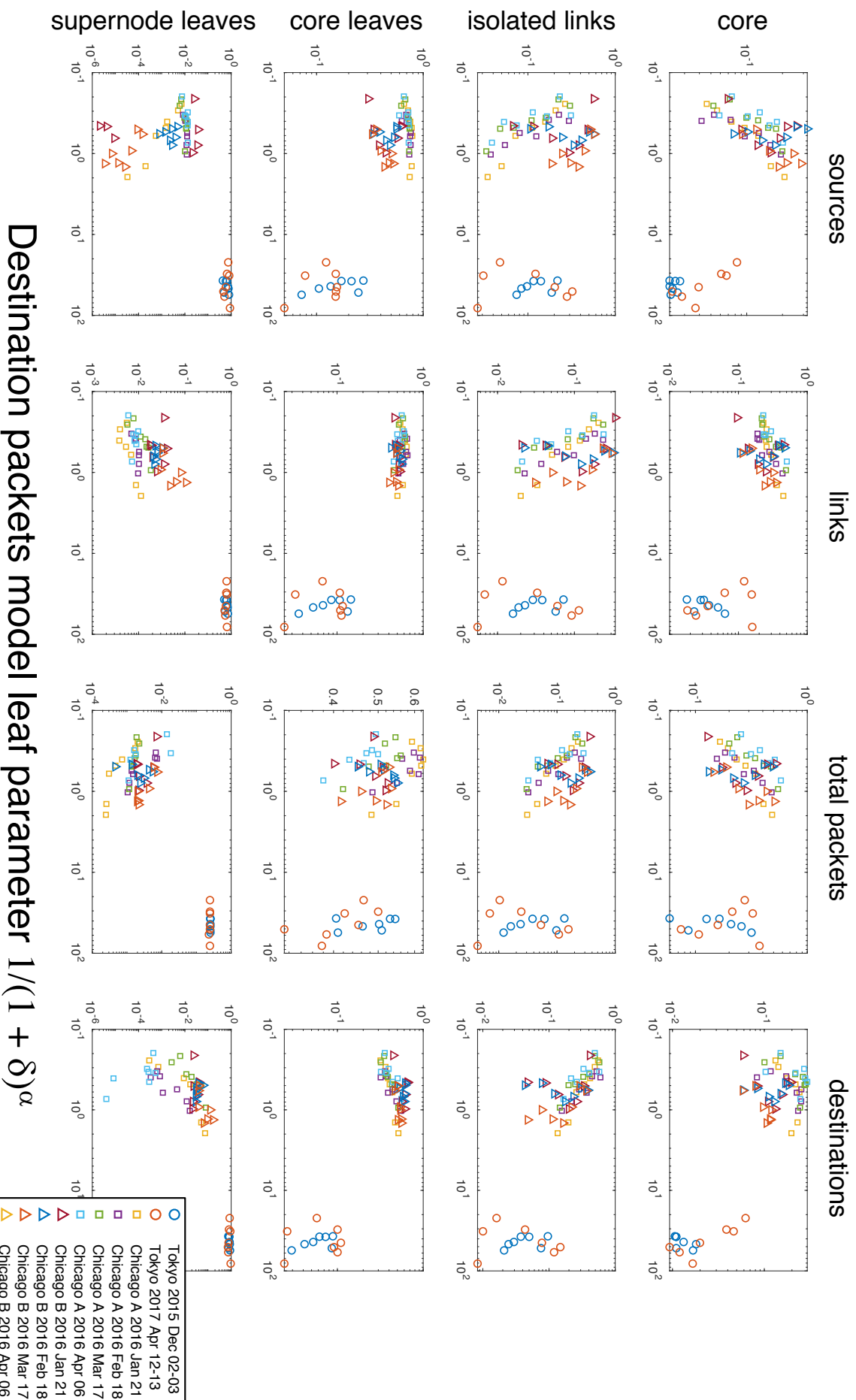
Fraction of total in:



Destination fan-in model leaf parameter  $1/(1 + \delta)^\alpha$

- Tokyo 2015 Dec 02-03
- Tokyo 2017 Apr 12-13
- Chicago A 2016 Jan 21
- Chicago A 2016 Feb 18
- Chicago A 2016 Mar 17
- Chicago B 2016 Apr 06
- Chicago B 2016 Jan 21
- Chicago B 2016 Feb 18
- Chicago B 2016 Mar 17
- Chicago B 2016 Apr 06
- Chicago A 2016 Mar 17
- Chicago A 2016 Apr 06
- Chicago B 2016 Jan 21
- Chicago B 2016 Feb 18
- Chicago B 2016 Mar 17
- Chicago B 2016 Apr 06
- Tokyo 2015 Dec 02-03
- Tokyo 2017 Apr 12-13
- Chicago A 2016 Jan 21
- Chicago A 2016 Feb 18
- Chicago A 2016 Mar 17
- Chicago B 2016 Apr 06
- Chicago B 2016 Jan 21
- Chicago B 2016 Feb 18
- Chicago B 2016 Mar 17
- Chicago B 2016 Apr 06
- △ Chicago A 2016 Mar 17
- △ Chicago A 2016 Apr 06
- △ Chicago B 2016 Jan 21
- △ Chicago B 2016 Feb 18
- △ Chicago B 2016 Mar 17
- △ Chicago B 2016 Apr 06
- △ Tokyo 2015 Dec 02-03
- △ Tokyo 2017 Apr 12-13
- △ Chicago A 2016 Jan 21
- △ Chicago A 2016 Feb 18
- △ Chicago A 2016 Mar 17
- △ Chicago B 2016 Apr 06
- △ Chicago B 2016 Jan 21
- △ Chicago B 2016 Feb 18
- △ Chicago B 2016 Mar 17
- △ Chicago B 2016 Apr 06

## Fraction of total in:



## S14 Memory and Computation Requirements

Processing 49.6 billion Internet packets with a variety of algorithms presents numerous computational challenges. Dividing the data set into combinable units of approximately 100,000 consecutive packets made the analysis amenable to processing on a massively parallel supercomputer. The detailed architecture of the parallel processing system and its corresponding performance are described in (25). The resulting processing pipeline was able to efficiently use over 10,000 processors on the MIT SuperCloud and was essential to this first-ever complete analysis of these data.

A key element of our analysis is the use of novel sparse matrix mathematics in concert with the MIT SuperCloud to process very large network traffic matrices. Construction and analysis of network traffic matrices of the entire Internet address space have been considered impractical for its massive size (18). Internet Protocol version 4 (IPv4) has  $2^{32}$  unique addresses, but at any given collection point only a fraction of these addresses will be observed. Exploiting this property to save memory can be accomplished by extending traditional sparse matrices so that new rows and columns can be added dynamically. The algebra of associative arrays (24) and its corresponding implementation in the Dynamic Distributed Dimensional Data Model (D4M) software library (d4m.mit.edu) allows the row and columns of a sparse matrix to be any sortable value, in this case character string representations of the Internet addresses (fig. S8). Associative arrays extend sparse matrices to have database table properties with dynamically insertable and removable rows and columns that adjust as new data is added or subtracted to the matrix. Using these properties, the memory requirements of forming network traffic matrices can be reduced at the cost of increasing the required computation necessary to resort the rows and columns. A network matrix  $\mathbf{A}_t$  with  $N_V = 100,000,000$  represented as an associative array typically requires 2 Gigabytes of memory. Complete analysis of the statistics and topologies

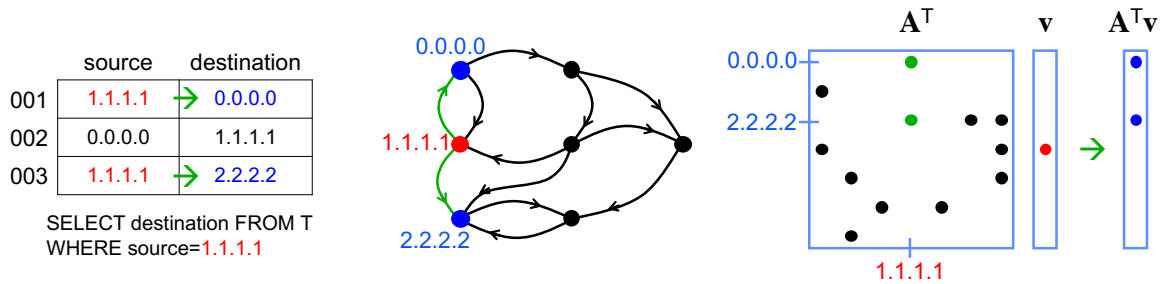


Figure S8: **Associative Arrays.** (left) Tabular representation of raw network traffic and corresponding database query to find all records beginning with source 1.1.1.1. (middle) Network graph highlighting nearest neighbors of source node 1.1.1.1. (right) Corresponding associative array representation of the network graph illustrating how the neighbors of source node 1.1.1.1 are computed with matrix vector multiplication.

of  $A_t$  typically takes 10 minutes on a single MIT SuperCloud Intel Knights Landing processor core. Using increments of 100,000 packets means that this analysis is repeated over 500,000 times to process all 49.6 billion packets. Using 10,000 processors on the MIT SuperCloud shortens the run time of one these analysis to approximately 8 hours. The results presenting here are the product of a discovery process that required hundreds of such runs that would not have been possible without these computational resources. Fortunately, the utilization of these results by Internet stakeholders can be significantly accelerated by creating optimized embedded implementations that only compute the desired statistics and are not required to support a discovery process (S63, S64).

## S15 Practical Implications

Measurements of internet traffic are useful for informing policy, identifying and preventing outages, defeating attacks, planning for future loads, and protecting the domain name system (S65). On a given day, millions of IPs are engaged in scanning behavior. Our improved models can aid cybersecurity analysts in determining which of these IPs are nefarious (S66), the distribution of attacks in particular critical sectors (S67), identifying spamming behavior (S68), how to vaci-

nate against computer viruses (*S69*), obscuring web sources (*S70*), identifying significant flow aggregates in traffic (*S71*), and sources of rumors (*S72*).

The results presented here have a number of potential practical applications for Internet stakeholders. The methods presented of collecting, filtering, computing, and binning the data to produce accurate measurements of a variety of network quantities are generally applicable to Internet measurement and have the potential to produce more accurate measures of these quantities. The accurate fits of the two parameter modified Zipf-Mandelbrot distribution offer all the usual benefits of low parameter models: measuring parameters with far less data, accurate predictions of network quantities based on a few parameters, observing changes in the underlying distribution, and using modeled distributions to detect anomalies in the data.

From a scientific perspective, improved knowledge of how Internet traffic flows can inform our understanding of how economics, topology, and demand shape the Internet over time. As with all scientific disciplines, the ability of theoreticians to develop and test theories of the Internet and network phenomena is bounded by the scale and accuracy of measured phenomena (*S73, S74, S75, S76*). The connections among dynamic evolution (*S77*), network topology (*S54*) (*S78, S79*), network robustness (*S80*), controlability (*S81*), community formation (*S82*), and spreading phenomena (*S83*) have emerged in many contexts (*S84, S85, S86*). Many first-principle theories for Internet and network phenomena have been proposed, such as Poisson models (*S3*), fractional Brownian motion (*S6*), preferential attachment (*9, 10*) (*S87, S88*), statistical mechanics (*S89*), percolation (*S90*), hyperbolic geometries (*S43, S44*), non-global greedy routing (*S45, S46, S47*), interacting particle systems (*S91*), higher-order organization of complex networks from graph motifs (*33*), and minimum control energy (*S92*). All of these models require data to test them. In contrast to previous network models that have principally been based on data obtained from network crawls from a variety of start points on the network, our network traffic data are collected from observations of network streams. Both viewpoints provide im-

portant network observations. Observations of a network stream provide complementary data on network dynamics and highlight the contribution of leaves and isolated edges, which are less sampled in network crawls.

The aggregated data set our teams have collected provide a unique window into these questions. The non-linear fitting techniques described are a novel approach to fitting power-law data and have potential applications to power-law networks in diverse domains. The model fit parameters present new opportunities to connect the distributions to underlying theoretical models of networks. That the model fit parameters distinguish the different collection points and are reflective of different network topologies in the data at these points suggests a deeper underlying connection between the models and the network topologies.

## Supplementary References

- [S1] M. Rabinovich and M. Allman, “Measuring the internet,” *IEEE Internet Computing*, vol. 20, no. 4, pp. 6–8, 2016.
- [S2] K. C. Claffy, H.-W. Braun, and G. C. Polyzos, “Tracking long-term growth of the nsfnet,” *Communications of the ACM*, vol. 37, no. 8, pp. 34–45, 1994.
- [S3] V. Paxson and S. Floyd, “Wide area traffic: the failure of poisson modeling,” *IEEE/ACM Transactions on Networking (ToN)*, vol. 3, no. 3, pp. 226–244, 1995.
- [S4] V. Paxson, “End-to-end routing behavior in the internet,” *ACM SIGCOMM Computer Communication Review*, vol. 26, no. 4, pp. 25–38, 1996.
- [S5] W. E. Leland, M. S. Taqqu, W. Willinger, and D. V. Wilson, “On the self-similar nature of ethernet traffic (extended version),” *IEEE/ACM Transactions on Networking (ToN)*, vol. 2, no. 1, pp. 1–15, 1994.

- [S6] W. Willinger, M. S. Taqqu, R. Sherman, and D. V. Wilson, "Self-similarity through high-variability: statistical analysis of ethernet lan traffic at the source level," *IEEE/ACM Transactions on Networking (ToN)*, vol. 5, no. 1, pp. 71–86, 1997.
- [S7] W. Willinger, R. Govindan, S. Jamin, V. Paxson, and S. Shenker, "Scaling phenomena in the internet: Critically examining criticality," *Proceedings of the National Academy of Sciences*, vol. 99, no. suppl 1, pp. 2573–2580, 2002.
- [S8] M. Faloutsos, P. Faloutsos, and C. Faloutsos, "On power-law relationships of the internet topology," in *ACM SIGCOMM computer communication review*, vol. 29-4, pp. 251–262, ACM, 1999.
- [S9] A. Medina, I. Matta, and J. Byers, "On the origin of power laws in internet topologies," *ACM SIGCOMM computer communication review*, vol. 30, no. 2, pp. 18–28, 2000.
- [S10] A. Broder, R. Kumar, F. Maghoul, P. Raghavan, S. Rajagopalan, R. Stata, A. Tomkins, and J. Wiener, "Graph structure in the web," *Computer networks*, vol. 33, no. 1-6, pp. 309–320, 2000.
- [S11] W. Willinger, D. Alderson, and J. C. Doyle, "Mathematics and the internet: A source of enormous confusion and great potential," *Notices of the American Mathematical Society*, vol. 56, no. 5, pp. 586–599, 2009.
- [S12] N. Spring, R. Mahajan, and D. Wetherall, "Measuring isp topologies with rocketfuel," *ACM SIGCOMM Computer Communication Review*, vol. 32, no. 4, pp. 133–145, 2002.
- [S13] L. Li, D. Alderson, W. Willinger, and J. Doyle, "A first-principles approach to understanding the internet's router-level topology," in *ACM SIGCOMM Computer Communication Review*, vol. 34, pp. 3–14, ACM, 2004.

- [S14] J. Heidemann, Y. Pradkin, R. Govindan, C. Papadopoulos, G. Bartlett, and J. Bannister, “Census and survey of the visible internet,” in *Proceedings of the 8th ACM SIGCOMM conference on Internet measurement*, pp. 169–182, ACM, 2008.
- [S15] A. Mahanti, N. Carlsson, A. Mahanti, M. Arlitt, and C. Williamson, “A tale of the tails: Power-laws in internet measurements,” *IEEE Network*, vol. 27, no. 1, pp. 59–64, 2013.
- [S16] M. Kitsak, A. Elmokashfi, S. Havlin, and D. Krioukov, “Long-range correlations and memory in the dynamics of internet interdomain routing,” *PloS one*, vol. 10, no. 11, p. e0141481, 2015.
- [S17] M. Lischke and B. Fabian, “Analyzing the bitcoin network: The first four years,” *Future Internet*, vol. 8, no. 1, p. 7, 2016.
- [S18] A. Dhamdhere and C. Dovrolis, “The internet is flat: modeling the transition from a transit hierarchy to a peering mesh,” in *Proceedings of the 6th International Conference*, p. 21, ACM, 2010.
- [S19] C. Labovitz, S. Iekel-Johnson, D. McPherson, J. Oberheide, and F. Jahanian, “Internet inter-domain traffic,” *ACM SIGCOMM Computer Communication Review*, vol. 41, no. 4, pp. 75–86, 2011.
- [S20] Y.-C. Chiu, B. Schlinker, A. B. Radhakrishnan, E. Katz-Bassett, and R. Govindan, “Are we one hop away from a better internet?,” in *Proceedings of the 2015 Internet Measurement Conference*, pp. 523–529, ACM, 2015.
- [S21] R. Fontugne, C. Pelsser, E. Aben, and R. Bush, “Pinpointing delay and forwarding anomalies using large-scale traceroute measurements,” in *Proceedings of the 2017 Internet Measurement Conference*, pp. 15–28, ACM, 2017.



- [S22] A. Dhamdhere, D. D. Clark, A. Gamero-Garrido, M. Luckie, R. K. Mok, G. Akiwate, K. Gogia, V. Bajpai, A. C. Snoeren, and K. Claffy, “Inferring persistent interdomain congestion,” in *Proceedings of the 2018 Conference of the ACM Special Interest Group on Data Communication*, pp. 1–15, ACM, 2018.
- [S23] J. Mirkovic, G. Bartlett, J. Heidemann, H. Shi, and X. Deng, “Do you see me now? sparsity in passive observations of address liveness,” in *Network Traffic Measurement and Analysis Conference (TMA), 2017*, pp. 1–9, IEEE, 2017.
- [S24] K. Cho, K. Fukuda, H. Esaki, and A. Kato, “The impact and implications of the growth in residential user-to-user traffic,” in *ACM SIGCOMM Computer Communication Review*, vol. 36, pp. 207–218, ACM, 2006.
- [S25] P. Borgnat, G. Dewaele, K. Fukuda, P. Abry, and K. Cho, “Seven years and one day: Sketching the evolution of internet traffic,” in *INFOCOM 2009, IEEE*, pp. 711–719, IEEE, 2009.
- [S26] R. Fontugne, P. Abry, K. Fukuda, D. Veitch, K. Cho, P. Borgnat, and H. Wendt, “Scaling in internet traffic: a 14 year and 3 day longitudinal study, with multiscale analyses and random projections,” *IEEE/ACM Transactions on Networking (TON)*, vol. 25, no. 4, pp. 2152–2165, 2017.
- [S27] J. Fan, J. Xu, M. H. Ammar, and S. B. Moon, “Prefix-preserving ip address anonymization: measurement-based security evaluation and a new cryptography-based scheme,” *Computer Networks*, vol. 46, no. 2, pp. 253–272, 2004.
- [S28] K. Cho, K. Fukuda, H. Esaki, and A. Kato, “Observing slow crustal movement in residential user traffic,” in *Proceedings of the 2008 ACM CoNEXT Conference*, p. 12, ACM, 2008.

- [S29] M. Allman, V. Paxson, and J. Terrell, “A brief history of scanning,” in *Proceedings of the 7th ACM SIGCOMM conference on Internet measurement*, pp. 77–82, ACM, 2007.
- [S30] K. Claffy, “Measuring the internet,” *IEEE Internet Computing*, vol. 4, no. 1, pp. 73–75, 2000.
- [S31] “[http://www.caida.org/data/passive/trace\\_stats/](http://www.caida.org/data/passive/trace_stats/).”
- [S32] D. Moore, C. Shannon, *et al.*, “Code-red: a case study on the spread and victims of an internet worm,” in *Proceedings of the 2nd ACM SIGCOMM Workshop on Internet measurement*, pp. 273–284, ACM, 2002.
- [S33] D. Moore, V. Paxson, S. Savage, C. Shannon, S. Staniford, and N. Weaver, “Inside the slammer worm,” *IEEE Security & Privacy*, vol. 99, no. 4, pp. 33–39, 2003.
- [S34] D. Moore, C. Shannon, G. M. Voelker, and S. Savage, “Internet quarantine: Requirements for containing self-propagating code,” in *INFOCOM 2003. Twenty-Second Annual Joint Conference of the IEEE Computer and Communications. IEEE Societies*, vol. 3, pp. 1901–1910, IEEE, 2003.
- [S35] C. Dovrolis, P. Ramanathan, and D. Moore, “What do packet dispersion techniques measure?,” in *INFOCOM 2001. Twentieth Annual Joint Conference of the IEEE Computer and Communications Societies. Proceedings. IEEE*, vol. 2, pp. 905–914, IEEE, 2001.
- [S36] C. Dovrolis, P. Ramanathan, and D. Moore, “Packet-dispersion techniques and a capacity-estimation methodology,” *IEEE/ACM Transactions On Networking*, vol. 12, no. 6, pp. 963–977, 2004.
- [S37] R. Prasad, C. Dovrolis, M. Murray, and K. Claffy, “Bandwidth estimation: metrics, measurement techniques, and tools,” *IEEE network*, vol. 17, no. 6, pp. 27–35, 2003.

- [S38] T. Karagiannis, A. Broido, M. Faloutsos, *et al.*, “Transport layer identification of p2p traffic,” in *Proceedings of the 4th ACM SIGCOMM conference on Internet measurement*, pp. 121–134, ACM, 2004.
- [S39] T. Karagiannis, A. Broido, N. Brownlee, K. C. Claffy, and M. Faloutsos, “Is p2p dying or just hiding?,” in *IEEE Global Telecommunications Conference, 2004. GLOBECOM’04.*, vol. 3, pp. 1532–1538, IEEE, 2004.
- [S40] T. Kohno, A. Broido, and K. C. Claffy, “Remote physical device fingerprinting,” *IEEE Transactions on Dependable and Secure Computing*, vol. 2, no. 2, pp. 93–108, 2005.
- [S41] D. Moore, C. Shannon, D. J. Brown, G. M. Voelker, and S. Savage, “Inferring internet denial-of-service activity,” *ACM Transactions on Computer Systems (TOCS)*, vol. 24, no. 2, pp. 115–139, 2006.
- [S42] H. Kim, K. C. Claffy, M. Fomenkov, D. Barman, M. Faloutsos, and K. Lee, “Internet traffic classification demystified: myths, caveats, and the best practices,” in *Proceedings of the 2008 ACM CoNEXT conference*, p. 11, ACM, 2008.
- [S43] D. Krioukov, F. Papadopoulos, A. Vahdat, and M. Boguñá, “Curvature and temperature of complex networks,” *Physical Review E*, vol. 80, no. 3, p. 035101, 2009.
- [S44] D. Krioukov, F. Papadopoulos, M. Kitsak, A. Vahdat, and M. Boguñá, “Hyperbolic geometry of complex networks,” *Physical Review E*, vol. 82, no. 3, p. 036106, 2010.
- [S45] M. Boguñá and D. Krioukov, “Navigating ultrasmall worlds in ultrashort time,” *Physical review letters*, vol. 102, no. 5, p. 058701, 2009.
- [S46] M. Boguna, D. Krioukov, and K. C. Claffy, “Navigability of complex networks,” *Nature Physics*, vol. 5, no. 1, p. 74, 2009.

- [S47] M. Boguná, F. Papadopoulos, and D. Krioukov, “Sustaining the internet with hyperbolic mapping,” *Nature communications*, vol. 1, p. 62, 2010.
- [S48] M. Kitsak, L. K. Gallos, S. Havlin, F. Liljeros, L. Muchnik, H. E. Stanley, and H. A. Makse, “Identification of influential spreaders in complex networks,” *Nature physics*, vol. 6, no. 11, p. 888, 2010.
- [S49] F. Papadopoulos, M. Kitsak, M. Á. Serrano, M. Boguná, and D. Krioukov, “Popularity versus similarity in growing networks,” *Nature*, vol. 489, no. 7417, p. 537, 2012.
- [S50] D. Krioukov, M. Kitsak, R. S. Sinkovits, D. Rideout, D. Meyer, and M. Boguñá, “Network cosmology,” *Scientific reports*, vol. 2, p. 793, 2012.
- [S51] A. Dainotti, A. Pescape, and K. C. Claffy, “Issues and future directions in traffic classification,” *IEEE network*, vol. 26, no. 1, 2012.
- [S52] L. Zhang, A. Afanasyev, J. Burke, V. Jacobson, P. Crowley, C. Papadopoulos, L. Wang, B. Zhang, *et al.*, “Named data networking,” *ACM SIGCOMM Computer Communication Review*, vol. 44, no. 3, pp. 66–73, 2014.
- [S53] V. Bharti, P. Kankar, L. Setia, G. Gürsun, A. Lakhina, and M. Crovella, “Inferring invisible traffic,” in *Proceedings of the 6th International Conference*, p. 22, ACM, 2010.
- [S54] P. J. Mucha, T. Richardson, K. Macon, M. A. Porter, and J.-P. Onnela, “Community structure in time-dependent, multiscale, and multiplex networks,” *science*, vol. 328, no. 5980, pp. 876–878, 2010.
- [S55] J. Karvanen and A. Cichocki, “Measuring sparseness of noisy signals,” in *4th International Symposium on Independent Component Analysis and Blind Signal Separation*, pp. 125–130, 2003.

- [S56] A. Soule, A. Nucci, R. Cruz, E. Leonardi, and N. Taft, “How to identify and estimate the largest traffic matrix elements in a dynamic environment,” in *ACM SIGMETRICS Performance Evaluation Review*, vol. 32, pp. 73–84, ACM, 2004.
- [S57] “NIST Digital Library of Mathematical Functions, Release 1.0.20 of 2018-09-15.” <http://dlmf.nist.gov/25.11>. F. W. J. Olver, A. B. Olde Daalhuis, D. W. Lozier, B. I. Schneider, R. F. Boisvert, C. W. Clark, B. R. Miller and B. V. Saunders, eds.
- [S58] A. Clauset, C. R. Shalizi, and M. E. Newman, “Power-law distributions in empirical data,” *SIAM review*, vol. 51, no. 4, pp. 661–703, 2009.
- [S59] X. Yu and T. Chu, “Link prediction from partial observation in scale-free networks,” in *Chinese Intelligent Systems Conference*, pp. 199–205, Springer, 2017.
- [S60] N. Saito, B. M. Larson, and B. Bénichou, “Sparsity vs. statistical independence from a best-basis viewpoint,” in *Wavelet Applications in Signal and Image Processing VIII*, vol. 4119, pp. 474–487, International Society for Optics and Photonics, 2000.
- [S61] M. Brbic and I. Kopriva, “ $\ell_0$ -motivated low-rank sparse subspace clustering,” *IEEE Transactions on Cybernetics*, pp. 1–15, 2018.
- [S62] H. D. Yaghoub Rahimi, Chao Wang and Y. Lous, “A scale invariant approach for sparse signal recovery,” *arXiv preprint arXiv:1812.08852*, 2018.
- [S63] A. X. Liu, C. R. Meiners, and E. Torng, “Tcam razor: A systematic approach towards minimizing packet classifiers in tcams,” *IEEE/ACM Transactions on Networking (TON)*, vol. 18, no. 2, pp. 490–500, 2010.

- [S64] A. X. Liu, C. R. Meiners, and E. Torng, “Packet classification using binary content addressable memory,” *IEEE/ACM Transactions on Networking*, vol. 24, no. 3, pp. 1295–1307, 2016.
- [S65] D. Clark *et al.*, “The 9th workshop on active internet measurements (aims-9) report,” *ACM SIGCOMM Computer Communication Review*, vol. 47, no. 5, pp. 35–38, 2017.
- [S66] S. Yu, G. Zhao, W. Dou, and S. James, “Predicted packet padding for anonymous web browsing against traffic analysis attacks,” *IEEE Transactions on Information Forensics and Security*, vol. 7, no. 4, pp. 1381–1393, 2012.
- [S67] M. Husák, N. Neshenko, M. S. Pour, E. Bou-Harb, and P. Čeleda, “Assessing internet-wide cyber situational awareness of critical sectors,” in *Proceedings of the 13th International Conference on Availability, Reliability and Security, ARES 2018*, (New York, NY, USA), pp. 29:1–29:6, ACM, 2018.
- [S68] O. Fonseca, E. Fazzion, I. Cunha, P. H. B. Las-Casas, D. Guedes, W. Meira, C. Hoepers, K. Steding-Jessen, and M. H. Chaves, “Measuring, characterizing, and avoiding spam traffic costs,” *IEEE Internet Computing*, vol. 20, no. 4, pp. 16–24, 2016.
- [S69] J. Balthrop, S. Forrest, M. E. Newman, and M. M. Williamson, “Technological networks and the spread of computer viruses,” *Science*, vol. 304, no. 5670, pp. 527–529, 2004.
- [S70] M. Javed, C. Herley, M. Peinado, and V. Paxson, “Measurement and analysis of traffic exchange services,” in *Proceedings of the 2015 Internet Measurement Conference*, pp. 1–12, ACM, 2015.
- [S71] K. Cho, “Recursive lattice search: Hierarchical heavy hitters revisited,” in *Proceedings of the 2017 Internet Measurement Conference*, pp. 283–289, ACM, 2017.

- [S72] R. Paluch, X. Lu, K. Suchecki, B. K. Szymański, and J. A. Hołyst, “Fast and accurate detection of spread source in large complex networks,” *Scientific reports*, vol. 8, no. 1, p. 2508, 2018.
- [S73] L. A. Adamic and B. A. Huberman, “Power-law distribution of the world wide web,” *science*, vol. 287, no. 5461, pp. 2115–2115, 2000.
- [S74] T. Bohman, “Emergence of connectivity in networks,” *evolution*, vol. 11, p. 13, 2009.
- [S75] M. P. Stumpf and M. A. Porter, “Critical truths about power laws,” *Science*, vol. 335, no. 6069, pp. 665–666, 2012.
- [S76] Y. Virkar and A. Clauset, “Power-law distributions in binned empirical data,” *The Annals of Applied Statistics*, pp. 89–119, 2014.
- [S77] G. Bianconi and A.-L. Barabási, “Competition and multiscaling in evolving networks,” *EPL (Europhysics Letters)*, vol. 54, no. 4, p. 436, 2001.
- [S78] S. Boccaletti, G. Bianconi, R. Criado, C. I. Del Genio, J. Gómez-Gardenes, M. Romance, I. Sendina-Nadal, Z. Wang, and M. Zanin, “The structure and dynamics of multilayer networks,” *Physics Reports*, vol. 544, no. 1, pp. 1–122, 2014.
- [S79] L. Lü, D. Chen, X.-L. Ren, Q.-M. Zhang, Y.-C. Zhang, and T. Zhou, “Vital nodes identification in complex networks,” *Physics Reports*, vol. 650, pp. 1–63, 2016.
- [S80] A. Li, S. P. Cornelius, Y.-Y. Liu, L. Wang, and A.-L. Barabási, “The fundamental advantages of temporal networks,” *Science*, vol. 358, no. 6366, pp. 1042–1046, 2017.
- [S81] Y.-Y. Liu and A.-L. Barabási, “Control principles of complex systems,” *Reviews of Modern Physics*, vol. 88, no. 3, p. 035006, 2016.

- [S82] M. Perc, J. J. Jordan, D. G. Rand, Z. Wang, S. Boccaletti, and A. Szolnoki, “Statistical physics of human cooperation,” *Physics Reports*, vol. 687, pp. 1–51, 2017.
- [S83] P. Holme, “Modern temporal network theory: a colloquium,” *The European Physical Journal B*, vol. 88, no. 9, p. 234, 2015.
- [S84] A.-L. Barabási, “Scale-free networks: a decade and beyond,” *science*, vol. 325, no. 5939, pp. 412–413, 2009.
- [S85] Z. Wang, C. T. Bauch, S. Bhattacharyya, A. d’Onofrio, P. Manfredi, M. Perc, N. Perra, M. Salathé, and D. Zhao, “Statistical physics of vaccination,” *Physics Reports*, vol. 664, pp. 1–113, 2016.
- [S86] C. J. Koliba, J. W. Meek, A. Zia, and R. W. Mills, *Governance networks in public administration and public policy*. Routledge, 2018.
- [S87] M. E. Newman, “Clustering and preferential attachment in growing networks,” *Physical review E*, vol. 64, no. 2, p. 025102, 2001.
- [S88] P. Sheridan and T. Onodera, “A preferential attachment paradox: How preferential attachment combines with growth to produce networks with log-normal in-degree distributions,” *Scientific reports*, vol. 8, no. 1, p. 2811, 2018.
- [S89] R. Albert and A.-L. Barabási, “Statistical mechanics of complex networks,” *Reviews of modern physics*, vol. 74, no. 1, p. 47, 2002.
- [S90] D. Achlioptas, R. M. D’souza, and J. Spencer, “Explosive percolation in random networks,” *Science*, vol. 323, no. 5920, pp. 1453–1455, 2009.
- [S91] C. G. Antonopoulos and Y. Shang, “Opinion formation in multiplex networks with general initial distributions,” *Scientific reports*, vol. 8, no. 1, p. 2852, 2018.



[S92] G. Lindmark and C. Altafini, “Minimum energy control for complex networks,” *Scientific reports*, vol. 8, no. 1, p. 3188, 2018.